An investigation of emerin and nuclear lamins: : Interactions, distribution, and role in cell cycle regulation, in cells derived from EDMD patients.

Maria, Choleza

To my parents...

Choleza Maria

An investigation of emerin and nuclear lamins: Interactions, distribution, and role in cell cycle regulation, in cells derived from EDMD patients.

A thesis submitted for the degree of Master in Science by research

September 2002

Abstract

Emery Dreifuss muscular dystrophy (EDMD) is caused by mutations either in the gene encoding emerin or in the gene encoding A-type lamins (lamins A and C). Several roles for emerin and A-type lamins have been proposed, including their involvement in nuclear structure, gene expression, cell cycle progression, and DNA replication. However, their functions are poorly understood and thus the mechanisms by which mutations cause different inherited diseases are not clear. In this project, the endogenous and exogenous distribution of emerin, and A- and B-type lamins in lymphoblasts and fibroblasts carrying mutations in emerin and A-type lamins have been investigated. For this purpose, antibodies against emerin, and A- and B-type lamins as well as GFP-, and DsRed- tagged fusion proteins (GFP-emerin, GFP-lamin A, and DsRed-lamin C) were used. From the immunofluorescence microscopy results of lymphoblasts, it is suggested that the distribution of emerin and lamins is possibly affected in these cells in EDMD. However, in fibroblasts there was no evidence of structural abnormality for the proteins investigated. The effects of emerin and A-type lamins mutations on growth and progression of cells through the cell cycle have also been investigated in fibroblasts of EDMD patients, using flow cytometry. The results obtained here suggest that emerin and lamin mutations may cause a cell cycle arrest at the G0 phase of the cycle.

An investigation of emerin and nuclear lamins: Interactions, distribution, and role in cell cycle regulation, in cells derived from EDMD patients.

Choleza Maria

School of Biology

University of Durham

A thesis submitted for the degree of Master in Science by research

September 2002

Declaration

I, Maria Choleza, hereby, certify that this thesis has been written by me, that it is the record of work carried out by me, and that it has not been submitted in any previous application for higher degree.

Statement of copyright

Acknowledgement

I am indebted to my supervisor, Prof. C. J. Hutchison for giving me this opportunity and for all his help and advice during the project. Many thanks to all the people in the lab for their help and support.

Table of contents

Introduction **10**

Muscular dystrophies 10

X-linked EDMD and emerin 12

Emerin structure 12

Gene mutations 13

Emerin localization 14

Emerin role and function 15

AD-EDMD and Lamins 17

Lamin mutations 17

Lamin structure 20

A-type and B-type lamins 21

Lamin role and function 24

Lamin interactions 29

Chapter 1 **32**

Introduction **32**

Materials and Methods **34**

Immunocytochemistry of LCLs 34

Cell lines and Cell culture 34

Antibodies 34

Immunofluorescence microscopy 37

Immunocytochemistry of fibroblasts 39

Cell lines and Cell culture 39

Plasmid construction 41

Transfections and Microscopy 41

Results **42**

Immunocytochemistry of LCLs 42

Lamin and emerin distribution in LCLs of patients with AD-EDMD 43

Lamin and emerin distribution in LCLs of patients with X-EDMD 46

Lamin and emerin distribution in LCLs of patients EDMD patients screened for lamin B1, LAP2beta and other proteins 46

Lamin and emerin distribution in LCLs of control cells 57

Immunocytochemistry of fibroblasts 60

Construction of DsRed-LaminC 60

Distribution of DsRed-LaminC in fibroblasts of AD-EDMD, and X-linked EDMD patients 60

Chapter 2 **68**

Introduction **68**

Materials and Methods **70**

Cell lines and Cell culture 70

DNA staining and FACS analysis 70

Results **72**

Discussion **90**

Immunocytochemistry of LCLs 90

Immunocytochemistry of fibroblasts 92

The nuclear lamina and cell cycle effects in EDMD cells 94

References 97

Tables and Illustrations

Table 1 Muscular dystrophies, their genes and loci 11

Table 2 Possible functions of emerin 18

Table 3 Lymphoblastoid cell lines and mutations 35

Table 4 Types of primary antibodies used 38

Table 5 Fibroblastic cell lines and mutations 40

Table 6 Lymphoblast staining of patients with AD-EDMD 44

Table 7 Lymphoblast staining of patients with X-linked EDMD 47

Table 8 Lymphoblast staining of patients with sporadic EDMD 51

Table 9 Lymphoblast staining of control cells 58

Figure 1 Schematic representation of somatic cell lamins. 22

Figure 2 The distribution of lamin C, Lamin A/C, lamin B1, lamin B2, and emerin in LCLs of AD-EDMD patients 45

Figure 3 The distribution of lamin C, Lamin A/C, lamin B1, lamin B2, and emerin in LCLs of X-EDMD patients 50

Figure 4 The distribution of lamin C, Lamin A/C, lamin B1, lamin B2, and emerin in LCLs of sporadic EDMD patients 56

Figure 5 The distribution of lamin C, Lamin A/C, lamin B1, lamin B2, and emerin in LCLs of normal individuals **59**

Figure 6 Gels illustrating the production of lamin C from the PCR reaction and the diagnostic cutting of the DsRed-LC construct **61**

Figure 7 The nucleotide sequence of DsRed-LC construct **62**

Figure 8 The distribution of GFP-emerin, DsRed-Lamin C, and GFP-Lamin A in X-EDMD Carrier's fibroblasts **63**

Figure 9 The distribution of GFP-emerin, DsRed-Lamin C, and GFP-Lamin A in X-EDMD1 patient's fibroblasts **64**

Figure 10 The distribution of GFP-emerin, DsRed-Lamin C, and GFP-Lamin A in X-EDMD2 patient's fibroblasts **65**

Figure 11 The distribution of GFP-emerin, DsRed-Lamin C, and GFP-Lamin A in AD-EDMD1 patient's fibroblasts **67**

Figure 12a The distribution of cells throughout the cell cycle in control cells at day 3 **73**

Figure 12b The distribution of cells throughout the cell cycle in control cells at day 5 **74**

Figure 12c The distribution of cells throughout the cell cycle in control cells at day 10 **75**

Figure 13a The distribution of cells throughout the cell cycle in X-EDMD1 patient at day 3 **76**

Figure 13b The distribution of cells throughout the cell cycle in X-EDMD1 patient at day 5 **77**

Figure 13c The distribution of cells throughout the cell cycle in X-EDMD1 patient at day 10 **78**

Figure 14a The distribution of cells throughout the cell cycle in X-EDMD Carrier at day 3 **80**

Figure 14b The distribution of cells throughout the cell cycle in X-EDMD Carrier at day 5 **81**

Figure 14c The distribution of cells throughout the cell cycle in X-EDMD Carrier at day 10 **82**

Figure 15a The distribution of cells throughout the cell cycle in X-EDMD2 patient at day 3 **84**

Figure 15b The distribution of cells throughout the cell cycle in X-EDMD2 patient at day 5 **85**

Figure 15c The distribution of cells throughout the cell cycle in X-EDMD2 patient at day 10 **86**

Figure 16a The distribution of cells throughout the cell cycle in AD-EDMD patient at day 3 **87**

Figure 16b The distribution of cells throughout the cell cycle in AD-EDMD patient at day 5 **88**

Figure 16c The distribution of cells throughout the cell cycle in AD-EDMD patient at day 10 **89**

Introduction

Muscular dystrophies

Muscular dystrophies are a large and heterogeneous group of inherited muscular disorders that are characterized by progressive weakness and wasting of muscles. Clinical and genetic findings from studies suggest that muscular dystrophies may be grouped into three broad categories: X-linked muscular dystrophies, autosomal dominant and autosomal recessive muscular dystrophies. In Table 1 some of the muscular dystrophies, their corresponding gene and its locus are listed.

Duchenne/Becker and Emery-Dreifuss muscular dystrophy (EDMD) are the two major types of dystrophies, both characterized by progressive skeletal muscle wasting and cardiac abnormalities (reviewed by Emery, 1989).

Duchenne/Becker muscular dystrophy is the most prevalent form of muscle disorder. The gene responsible for this disorder and its product, dystrophin, were identified in late 1980's. Dystrophin is a large cytoskeletal/plasma membrane-associated protein expressed in muscle and brain. It localizes at the inner face of the sarcolemma and forms part of a glycoprotein complex that links actin to the extracellular matrix. Studies of the genes encoding the proteins of the complex have provided evidence suggesting that the integrity of the dystrophin-glycoprotein complex is of great importance to maintaining the integrity of the membrane during contraction and relaxation of the muscle (reviewed by Betto et al., 1999).

EDMD is quite distinct from all other forms of muscular dystrophy. The clinical features of the disorder have an onset in early childhood and a slow progression thereafter. EDMD is characterized by a triad of symptoms: (i) early contractures of the elbows, Achilles tendons and posterior neck, (ii) slow, progressive muscle weakening and wasting specifically localized in the humero-peroneal muscles, and (iii) cardiac conduction defects

Table 1. Muscular dystrophies, their genes and loci.

Muscular dystrophies	Inheritance	Gene locus	Gene symbol	Gene product
Duchenne/Becker	XR	Xp21.2	DMD	Dystrophin
Emery-Dreifuss	XR	Xq28	XEMD	Emerin
Emery-Dreifuss	AD	1q21	ADEMD	Lamin A/C
Fascio-scapulo-humeral	AD	4q35	FSHD	
Limb-girdle	AD	5q22-q34	LGMD1A	
	AD	1q11-21	LGMD1B	
	AD	3p25	LGMD1C	Caveolin-3
	AR	15q15-q21	LGMD2A	Calpain 3
	AR	2p13	LGMD2B	Dysferlin
	AR	13q12	LGMD2C	γ-sarcoglycan
	AR	17q12-q21	LGMD2D	α-sarcoglycan
	AR	4q12	LGMD2E	β-sarcoglycan
	AR	5q33-q34	LGMD2F	δ-sarcoglycan
	AR	17q11-q12	LGMD2G	
	AR	9q31-q34	LGMD2H	
Distal myopathy (Miyoshi myopathy)	AR	2p12-14	MM	Dysferlin
Distal myopathy	AD	14	MPD1	
Bethlem myopathy	AD	21q22	COL6A1	Collagen VI a1
			COL6A2	Collagen VI a2
	AD	2q37	COL6A3	Collagen VI a3
Epidermolysis bullosa and muscular dystrophy	AR	8q24-qter	MD-EBS	Plectin

with conduction block. More than 40% of EDMD patients have a high risk of sudden death by heart block or develop a progressive cardiac failure. However, cardiac involvement in affected individuals is usually evident by the age of 30 and if diagnosed at an early stage, the cardiac defect can be cured by insertion of a pacemaker (Emery, 1989, 2000; Toniolo et al., 1998; Toniolo and Minetti, 1999).

X-linked EDMD and Emerin

Two forms of EDMD have been described. An X-linked recessive form and an autosomal dominant form, showing similar to identical clinical phenotypes (Morris and Manilal, 1999). The X-linked ED muscular dystrophy was first reported by Dreifuss and Hogan as a benign form of Duchenne muscular dystrophy. However it later became evident that this disease with the quite unusual symptoms was distinct from the Duchenne/Becker one and was given the term Emery-Dreifuss muscular dystrophy.

The X-linked recessive form arises from mutations in the gene encoding emerin protein (Bione et el., 1995). The identification of the gene responsible for the disorder in 1994 confirmed that the X-linked EDMD is indeed distinct from other muscular dystrophies (Bione et al., 1994). The gene locus for X-linked EDMD was mapped to the subchromosomal region Xq28 by linkage studies (Yates et al., 1993), and the corresponding gene designated as *STA* was identified by positional cloning (Bione et al., 1994). The gene is very small, only 2,100bp in length, and consists of six exons with an mRNA of 1.3kb. This mRNA encodes a serine-rich protein of 254 amino acids (aa) with a Mr of 28,993, named emerin.

Emerin Structure

Structural analysis has shown that emerin is a type II integral protein of the inner nuclear membrane (INM), and belongs to a group of integral membrane proteins that

include lamina-associated proteins (LAP1, LAP2) and the lamin B receptor (Morris and Manilal, 1999). It has a short hydrophobic transmembrane region 11 residues from the carboxyl terminus which contains the localization signal to the INM (Ostland et al., 1999). It also has a long hydrophilic N-terminal domain, which contains 22 putative phosphorylation sites for a range of kinases (Bione et al., 1996). The amino terminal domain, which extends into the nucleoplasm, has been shown to interact with non-membrane insoluble elements, probably components of the nuclear lamina and chromatin (Manilal et al., 1996).

Although emerin does not have an overall homology to any known proteins, aa sequences of both its N- and C-terminal regions have some similarities to thymopoietins (TP). TPβ, one of the three isoforms of TP has been shown to be identical to LAP2 (Harris et al., 1995). Moreover, emerin possesses two regions of homology to LAP2: a 39-residue region in its amino-terminal domain and the last 34 residues in the carboxyl-terminal domain, are both 41% identical to similarly positioned residues in LAP2 (Bione et al., 1994, Furukawa et al., 1995).

Gene Mutations

Until now, 63 mutations in the gene encoding emerin have been reported in the Mutation Database available at OMIM (http://www.path.cam.ac.uk/emd/mutation.html). Mutations occur homogeneous throughout the gene and there is no evidence of mutational 'hot spots'. The most common mutations reported are point mutations (49%) or small deletions (33%) / insertions (10%). Moreover, some point mutations (14%) were found in the splice junctions. Most mutations (63%) introduce premature stop codons in the open reading frame (ORF), and therefore, no functional protein is being synthesized (Manilal et al., 1996; Yates et al., 1999). A relatively small percentage of mutations (8%) occur in the starting codon (ATG), probably preventing the initiation of translation. In addition, a small

but significant number of mutations on the gene have been reported which result in modified emerin production (Yates et al., 1999). Interestingly, patients have been reported that carry point mutations or deletions/insertions in the last exon and in which emerin lacks the C-terminal part that contains the transmembrane domain of the protein. Some of these patients completely lack emerin, demonstrating thus the importance of the C-terminal domain for cellular localization and stability of the protein (Nagano et al., 1996; Manilal et al., 1998). Missense mutations and in-frame deletions described in patients also imply the importance of the molecular structure of emerin. In spite of the different mutations in the emerin gene, giving rise to a large number of different effects on the expression of the protein, the clinical features of all the EDMD patients are similar.

Emerin Localization

Although the clinical features associated with EDMD are specific and restricted, emerin expression is not restricted to the tissues which are clinically affected but is present in all other tissues studied so far (Manilal et al., 1996; Nagano et al., 1996; Manilal et al., 1997; Mora et al., 1997). Immunological staining with antisera raised against different regions of emerin demonstrated that in normal cells the protein is localized at the nuclear rim in all tissues (Manilal et al., 1996; Nagano et al., 1996), in the intercalated discs of cardiac muscle cells (Cartegni et al., 1997), and in the endoplasmic reticulum (ER) of skeletal muscle cells (Fairley et al., 1999). Subcellular fractionation experiments also demonstrate that emerin localizes to the nuclear envelope in normal muscle, while they show that in EDMD muscle cells with nonsense mutations in the emerin gene, emerin is absent (Manilal et al., 1996, Nagano et al., 1996). In the same experiments, a small proportion of the protein was also found in the microsomal fraction which demonstrate association with cytoplasmic membranes and possibly transport to the nucleus through the ER (Manilal et al., 1996). Cartegni et al., in 1997 reported the additional presence of emerin

at the intercalated discs in heart and cultured rat cardiomyocytes and suggested that cardiac conduction defects in EDMD might be explained by this additional localization of emerin. In relation to that, contractures and muscle wasting could also be accounted for if emerin was present at the myotendinous junctions as well, a structure related to the intercalated discs. However, later experiments showed that rabbit antisera can stain non specifically the intercalated discs and that both affinity-purified rabbit antibodies and monoclonal anti-emerin antibodies stain the nuclear membrane but not the discs in the heart (Manilal et al., 1999).

Emerin Role and Function

The role of emerin in the INM is not completely understood yet. A characteristic feature of emerin as was mentioned earlier is the high content of serine residues which can be phosphorylated/dephosphorylated by various protein kinases to create NE membrane bound/soluble emerin (Tsuchiya and Arahata, 1997). Studies have revealed that full size, normal emerin can occur in four different phosphorylated forms three of which appear to be associated with the cell cycle. The mutant forms of the protein on the other hand, can occur not only in four but in a large number of phosphorylated forms (Ellis et al., 1998). These studies suggest that emerin's correct phosphorylation and thus localization at the INM is essential for its normal function.

The functions of the integral membrane proteins in the INM in which emerin belongs are also not known yet. The experimental evidence available suggests that their function is closely related to the maintenance of the nuclear structure and architecture (Gerace and Foisner, 1994). Since skeletal and cardiac muscles and tissues surrounding joints are continuously subjected to vigorous movements, the mechanical stability of the nuclear membrane as well as the interactions with integral membrane proteins might be essential.

The similarity in molecular topology, ubiquitous expression and nuclear membrane localization as well as sequence homology between emerin and TPβ/LAP2, suggests that the two proteins are functionally related. Nuclear envelope proteins have been shown to interact with lamins and chromosomes, and binding is reported to be modulated by mitotic phosphorylation (Foisner and Gerace, 1993). Mechanical connections between integrins, cytoskeletal filaments and cytoplasm that stabilize nuclear structure have also been demonstrated (Maniotis et al., 1997). Finally, emerin is found at intranuclear sites where it colocalizes with the nuclear lamins and binds strongly to several yet unidentified insoluble matrix components (Ellis et al., 1998; Manilal et al., 1998; Squarzoni et al., 1998).

Three out of the four of emerin's different phosphorylated forms appear to be associated with the cell cycle. Data suggests that emerin may be involved in disassembly and reformation of the nuclear membrane during mitosis, as well as in maintenance of the nuclear membrane-chromatin organization structure during interphase. However, the viability of cells without emerin shows that it is not essential. More specifically, during mitosis emerin becomes dispersed throughout the cell, no longer colocalizing with the lamins. After mitosis and during the reassembly of the nuclei, a number of events take place such as targeting of the nuclear membrane to chromosomes, membrane fusion, nuclear pore complex (NPC) formation, lamina assembly and chromatin decondensation. LAPs and LBR are shown to be involved in the targeting of the nuclear membrane to chromosomes. Although their exact role is not specified, at late anaphase when the chromosomes are first enveloped with membranes, these proteins are traced at the chromosome surfaces at high concentrations (Ellenberg et al., 1997).

Experiments conducted on the basis of the above revealed that emerin is focally accumulated in the nuclear membranes of late telophase cells participating in the reconstitution of membranes around the daughter nuclei. Emerin co-localizes with Lamin

A/C, and is concentrated in some areas of the mitotic spindle and in the mid-body of mitotic cells (Manilal et al., 1998a; Dabauvalle et al., 1999). This indicates that emerin is involved in cell cycle dependant events and in the reorganization of the nuclear envelope at the end of mitosis. The phosphorylation of emerin may be involved in controlling these events.

Although the function of emerin is still unknown, the clinical, physiological and pathological changes are certainly caused by the deficiency of the protein in X-EDMD, and presumably by emerin-interacting molecule(s) in AD-EDMD. Possible functions of emerin are listed in Table 2.

AD-EDMD and Lamins

The rarer form of EDMD, autosomal dominant EDMD (AD-EDMD) has been described recently. The gene responsible for this form of the disorder has been identified at 1q21.3 (Bonne et al., 1999). It (LMNA) encodes two components of the nuclear lamina, lamins A and C of about 60-75kDa size, by alternatively splicing (Fisher et al., 1986; Lin and Woman, 1993; Bonne et al., 1999).

Lamin Mutations

Mutations in the LMNA gene in AD-EDMD can not be detected by immunohistochemistry (Bonne et al., 1999; Toniolo and Minetti, 1999), and diagnosis depends on mutation analysis facilitated by oligonucleotide microassay techniques (Hacia and Collins, 1999). One large AD-EDMD family has a mutation that produces a very early stop codon and thus a truncated lamin A/C composed of only the five amino-terminal amino acids (Bonne et al., 1999). Missense mutations in the head and in the tail domains resulting in amino acid changes in highly conserved residues were found in additional families. Immunostaining of nuclei from AD-EDMD demonstrated that both emerin and

Table 2. Possible functions of emerin

1. Mechanical stability of the nuclear membrane and interaction with integral membrane proteins
2. Regeneration of muscle fiber
3. Regulation of gene expression and chromosome organization
4. In heart, emerin localization to desmosomes and fasciae adherents could account for the characteristic conduction defects

lamin A/C are present in these nuclei (Toniolo and Minetti, 1999). This suggests that AD-EDMD is caused by haploinsufficiency for lamin A/C. Interestingly, another type of muscular dystrophy, the autosomal dominant form of limb-girdle muscular dystrophy with cardiac involvement, may be allelic with and therefore a variant of AD-EDMD (Van der Kooi et al., 1997). Furthermore, missense mutations in the rod domain in the LMNA gene result in dilated cardiomyopathy with conduction defects but no skeletal myopathy (Fatkin et al., 1999). Finally, LMNA mutations have been identified as the cause of Dunnigan-type familiar partial lipodystrophy associated with diabetes and coronary artery disease (Cao and Hegele, 2000).

The properties of the mutant lamins that cause muscular dystrophy, lipodystrophy and dilated cardiomyopathy are not known. In a study conducted recently (Ostlund et al., 2001), fifteen mutant forms of lamin A found in patients affected by the above diseases were investigated by transfections in C2C12 myoblasts. In four of these mutants immunofluorescence microscopy revealed decreased nuclear rim staining and formation of intranuclear foci. The distribution of endogenous lamin A/C, lamin B1 and B2 was also affected in these four mutants resulting in accumulation of the proteins inside the foci. In addition, in three of these mutants emerin was lost from the nuclear envelope. The results suggest that some but not all the mutations occurring in lamin A can disrupt the endogenous lamina and alter emerin localization.

In agreement to that, it has been reported that some point mutations in lamin A/C gene that cause dilated cardiomyopathy and AD-EDMD modify the assembly properties of lamin A and lamin C and cause partial mislocalization of emerin in HeLa cells. Moreover, these mutations also cause significant changes in the molecular organization of the nuclear periphery (Raharjo et al., 2001). On the other hand, it has also been shown that R482Q and R482W mutations in lamin A do not involve loss of ability to form a nuclear lamina or to

interact with emerin (Holt et al., 2001; Raharjo et al., 2001). Interestingly, in another study involving these two mutations (Vigouroux et al., 2001), a subpopulation of cells carrying these mutations showed nuclear envelope herniations lacking B-type lamins, NPCs, Lap2β and chromatin. Furthermore, abnormal blebbing nuclei with a disorganized peripheral meshwork containing A-type lamins, emerin, and A-type lamin binding proteins were also observed, while the nuclear envelope was reported to have become more fragile.

Lamin Structure

Analysis of cDNA sequences that encode nuclear lamins has shown that lamins are closely related to the endoplasmic intermediate filament (IF) multi-gene protein family (Fisher et al., 1986), and are therefore classified as type V intermediate filaments (Quinlan et al., 1995). Structurally, IF proteins have a primary sequence consisting of a highly conserved central α-helical "rod" domain flanked by less conserved globular "head" and "tail" domains (Heins and Aebi, 1994). The rod domain in vertebrate endoplasmic IF proteins is in most cases 310 aa in length, although some IF proteins can possess slightly smaller or larger rod domains (Hess et al., 1998; Wallace et al., 1998). The rod domain can be divided into three or four α-helical segments, coil 1a, coil 1b, coil 2a, and coil 2b, which are separated by non-a-helical linker sequences. Figure 1 shows a schematic representation of somatic cell lamins.

In nuclear lamins the rod domain is 352 aa long, i.e. 42 aa longer than other IF proteins. The extra residues consist of six heptad repeats with α-helical properties located in coil 1b (Weber et al., 1989a). It is interesting to note that invertebrate IF proteins also contain this 42 aa insert, implying thus that they are the precursor of lamins and that cytoplasmic IF proteins have evolved from lamins by the loss of that 42 aa insert (Way et al., 1992).

Another difference between nuclear lamins and cytoplasmic IF proteins is that the former have a nuclear localization signal (NLS) in their tail domains adjacent to the α-helical rod domain (the exact position of the NLS within the tail domain varies between different lamins), and a COOH-terminal sequence motif CaaX (C, cysteine; a, any aliphatic amino acid; X. any amino acid) (Moir et al., 1995).

The NLS facilitates the transport of the lamins to the nucleus and is homologous to the prototype NLS of the simian virus 40 large T antigen. The CaaX motif is required for farnesylation of the C-terminal cysteine that eventually leads to proteolytic cleavage of the C-terminal aaX residues and carboxy-methylation of the cysteine residue (reviewed within Vaughan et al., 2000b). The CaaX modifications and more specifically the added hydrophobic phenyl moiety is thought to be important for the targeting and anchorage of lamins to the nuclear membrane (Vorburger et al., 1989).

A-type and B-type Lamins

The nuclear envelope (NE) creates a compartment within the interphase cell in which DNA replication, transcription and RNA processing are regulated independently of translation. It consists of 4 main structures; the inner nuclear membrane (INM) and the outer nuclear membrane (ONM), the nuclear pore complexes (NPCs) and the nuclear lamina (Hutchison et al., 1994). Lamins are the major component of the nuclear lamina and in addition they also form intra-nuclear structures, as well as trans-nuclear tube-like structures (Bridges et al., 1993; Moir et al., 1994; Fricker et al., 1997). Two main types of lamins are known in mammals; A-type and B-type. A-type lamins, lamin A, C, and AΔ10, are the alternatively spliced products of the same gene, Lamin A/C (Fisher et al., 1986; Lin and Worman, 1993; Furakuwa et al., 1994; Machiels et al., 1996). B-type lamins on the other hand which include B1, B2 and B3 lamins, are encoded by distinct genes (Pollard et al., 1990; Biamonti et al., 1992).

Fig.1. Schematic representation of somatic cell lamins. Rectangles represent α-helical coiled-coil domains. The shaded area in coil 1b illustrates the position of the heptad repeat.

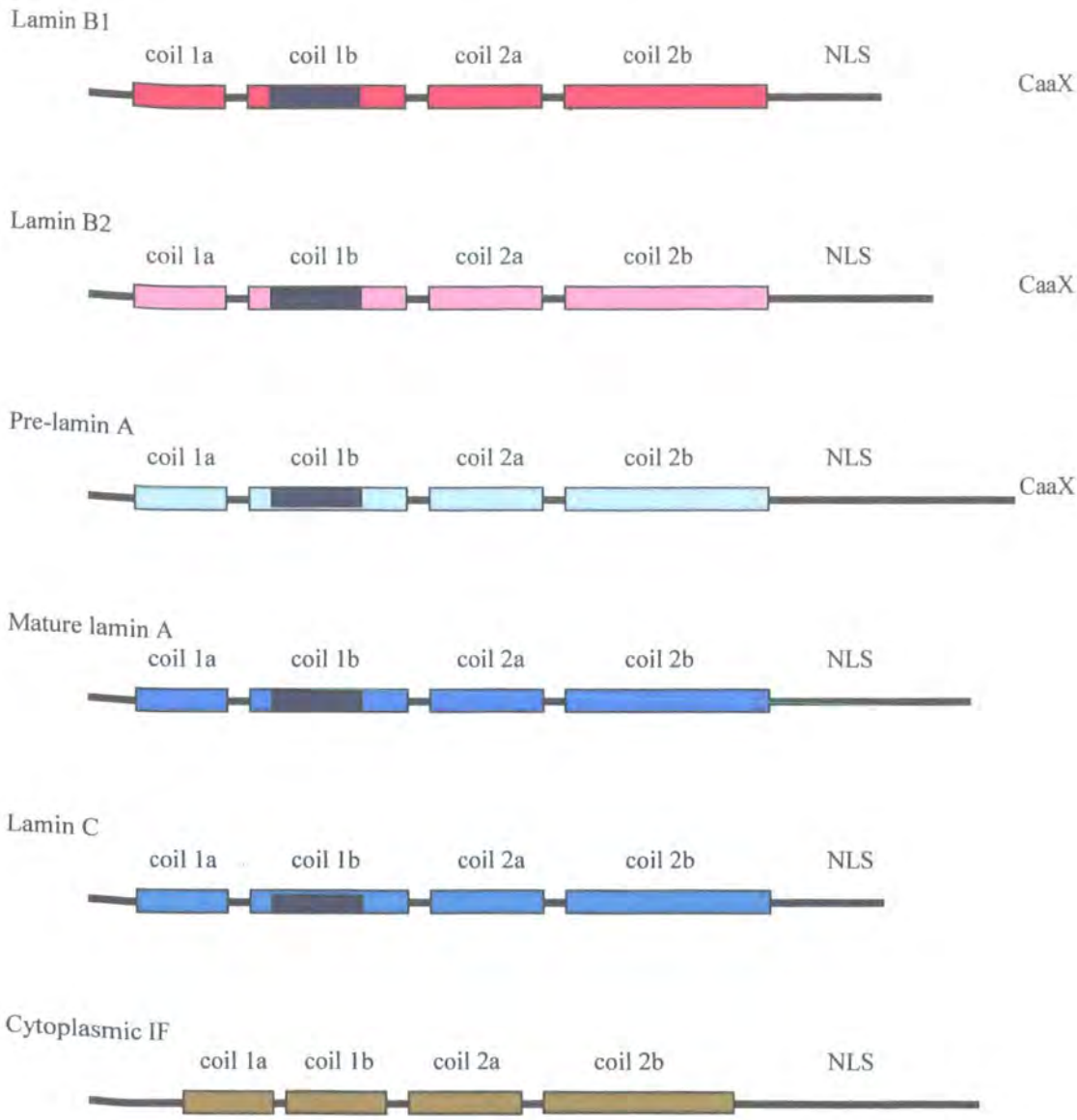

A-type and B-type lamins differ in several respects including their post-translational processing, behaviour at mitosis, and expression during differentiation (Gerace and Blobel, 1980; Farnsworth et al., 1989). More specifically, B-type lamins remain farmesylated throughout their lifetime, while A-type lamins are processed further. The C-terminal 15 residues of lamin A including the phenyl tail are removed by proteolytic cleavage to yield mature lamin A (Sasseville and Raymond, 1995). The retention of CaaX modifications confers different biochemical properties onto lamins.

The different post-translational processing of A- and B-type lamins may provide an explanation for their different behaviour at mitosis when nuclear and some cytoplasmic IFs are disassembled as a result of phosphorylation (Foisner, 1997). More specifically, during mitosis, the NE together with the lamina is disassembled and reassembled. Data from in vivo and in vitro assays suggest that the mitotic CDC2 kinase, protein kinase C (PKC), and cyclic-AMP-dependent kinase (PKA) phosphorylation sites are important in lamin assembly as well as disassembly (Moir et al., 1995). The disassembly of the lamina is thought to take place by the dissociation from the NE of A-type lamins followed by B-type lamins (Georgatos et al., 1997). Cdk1 complexed to cyclin B seem to be the main kinases responsible for lamin filament depolymerisation (reviewed in Moir et al., 1995). Phosphorylation sites for Cdk1 are located within the C-terminal domains of both types of lamins and more particularly at the end of coil 2, as well as within the N-terminal domain, adjacent to coil 1a of the rod domain. After disassembly of the NE and during mitosis, lamin A and lamin C probably form dimers and/or tetramers and remain 'soluble'. In contrast, B-type lamins generally remain most of the time attached to nuclear membrane vesicles (Gerace and Blobel, 1980).

Protein phosphatases have been implicated in lamina assembly (Murphy et al., 1995). In addition, phosphorylation by PKC at sites adjacent to the NLS can influence the

amount of lamins entering the nucleus, and therefore the availability of lamina's 'building blocks' (Hennekes et al., 1993). In contrast, PKA facilitates the incorporation of new lamin subunits into the lamina during nuclear growth (Peter et al., 1990). Finally, dephosphorylation by PP1a at CDK1 sites can influence the initial rate of lamin filament at telophase (Thompson et al., 1997).

B-type lamins are ubiquitous components of all cells. They are present in all embryonic and nucleated somatic cells, although different cells may express different B-type lamins (Furukawa and Hotta, 1993). In mammalian somatic cells the most common B-type lamins present are lamins B1 and B2 (Broers et al., 1997). A-type lamins on the other hand seem to be related to differentiation. They are present only in differentiated cells and tissues (Rober et al., 1989, 1990), and are observed in embryos at the time of differentiation.

Lamin Role and Functions

The functions of the nuclear lamins still remain unknown. It has been speculated however that they are involved in transcription regulation, chromatin organization, cell cycle progression and terminal differentiation.

Evidence from a number of laboratories suggests that lamins are required for DNA replication. Investigation of the involvement of lamins in DNA synthesis has made use of deletion mutants of Xenopus lamin B1 (Ellis et al., 1997) and human lamin A (Spann et al., 1997) on nuclei assembled in Xenopus egg extracts. Results from these investigations concluded that both lamin mutants which lack the N-terminal globular head domain leading to the creation of dominant negative proteins, are capable of preventing lamina assembly, disrupting a preformed lamina at S-phase nuclei and inhibiting DNA synthesis. In the case of lamin A mutant, the organization of some replication fork proteins was disrupted. The replication factor complex (RFC) and the proliferating cell nuclear antigen (PCNA) under

such conditions were found within intranuclear aggregates, co-localizing with the endogenous lamin B3 sequestered by the headless lamin A. This data is consistent with the observation that B-type lamins colocalize with centres of DNA replication in cultured mammalian cells during mid to late S-phase (Moir et al., 1994; Izumi et al., 2000). This data suggests that B-type lamins may function as a scaffold on which the DNA replication complexes are formed. The Xenopus minichromosome maintenance complex factor 3 (XMCM3), the Xenopus origin replication complex factor 2 (XORC2) and the DNA polymerase α however which are involved in the initiation of DNA synthesis, appeared to be unaffected. These observations imply that a properly assembled nuclear lamina is essential for the elongation phase of replication but not for the assembly of pre-replication complexes (Spann et al., 1997; Moir et al., 2000). In contrast to that, in another similar set of experiments involving lamin B1 mutants replication (elongation) was not blocked once sites of replication were established, although the lamina was disrupted (Ellis et al., 1997). These results suggest that lamina assembly is required to establish replication centres but is not essential for their maintenance and function.

Other studies suggest that nuclear lamins play a more indirect role in DNA replication. After an ultrastructural study of sperm pronuclear assembly Zhang and co-workers in 1996 suggested that the nuclear matrix consists of two filamentous structures; lamin filaments that contain lamin B3, and core filaments of the internal nuclear matrix that do not contain lamin B3 (Zhang et al., 1996). Furthermore, it was also suggested that the normal assembly of the nuclear matrix filaments and thus the nuclear matrix depends on correct assembly of the lamina although lamin B3 is not present in the core filaments. Because the nuclear matrix may support DNA replication centres, nuclear lamina assembly is required. In another study, a nuclear-free system in which DNA replication was initiated on chromosomal DNA added to concentrated nuclear extracts activated by cyclin E/Cdk2

was developed (Walter et al., 1998). In this case it was thought that the high concentration of replication factors in the nucleoplasmic extract overcomes the need of a NE and lamina. It is therefore implied that the role of lamina in DNA replication is indirect and that its function involves efficient nuclear transport and concentration of the replication factors inside the nucleus.

In agreement with the above are experiments in which the depletion of a nuclear pore complex protein or the addition of a nuclear transport inhibitor blocks replication (Powers et al., 1995; Walter et al., 1998). Initiation of DNA replication in in vitro assembled nuclei has also been reported to be size dependent (Hutchison et al., 1994), and lamin deficient nuclei are shown to arrest for nuclear growth at a size smaller than that required for initiation (Ellis et al., 1997).

The biochemical properties of the lamina and its association with the inner face of the nuclear membrane and the pores suggests that the lamina provides structural support for the NE (Moir et al., 1995). Nuclei assembled in vitro under lamin depleted conditions are fragile and easily broken (Moir et al., 1995). Perhaps the most convincing example demonstrating the importance of lamins for the nuclear structure is that of a mouse model for EDMD created by functional knockout of the lamin A/C gene (Sullivan et al., 1999). Lamin A/C null mice show no difference from normal mice at birth. However, after 3-4 weeks they develop severe muscle wasting and contractures similar to that of EDMD, while they die after 8 weeks of birth. In cells lacking lamin A/C nuclei are reported to be misshapen while there is a severe ultrastructural damage. Furthermore, nuclei appear to have herniations where the envelope pulls away from the chromatin, at which sites lamin B2, LAP2 and pore complexes are disrupted.

The first genetic evidence for the role of lamins in NE organization was provided by Lenz-Böhme et al., 1997. In Drosophila melanogaster two lamin genes are known coding

for lamins DmO and C which have some similarities to vertebrate B-type and A-type lamins respectively (reviewed in Stuurman et al., 1998). Insertional mutation in the DmO lamin gene (<20% of lamin expression) results in a severe mutant phenotype with defective NE (abnormalities in the initial assembly of the NE and NPC distribution) and reduced viability (Lenz- Böhme et al., 1997). Subsequent studies reported that flies homozygous for the lamin DmO gene mutations have aberrant nuclear structure and die after 9 to 14 hours of development, a time at which the maternal lamin DmO is diluted (Harel et al., 1998). These results suggest that the main function of lamins is in stabilizing the NE.

Recent studies have showed that the lamins are also important in NE assembly. NE assembly includes the targeting and fusion of membrane vesicles to the surfaces of decondensing chromosomes, the assembly of NPCs, and the repolymerisation of the lamina. Studies demonstrate that lamins have an important role in targeting nuclear vesicles to chromatin after mitosis (Gant and Wilson, 1997). In one such study lamins B2 and B3 in Xenopus were functionally depleted from egg extracts by the use of antibodies and that inhibited nuclear membrane assembly (Dabauvalle et al., 1991). Similarly, in Drosophila embryo cell-free system it was shown that antibody depletion of lamin Dm1 blocked binding of NE vesicles to chromatin while addition of purified interphase lamin Dm1 and Dm2 isoforms or undepleted cytosol restored the binding (Ulitzur et al., 1992, 1997). These results however are contradicted by a series of other experiments. For instance, in sea urchin egg extracts, depletion of lamin B did not seem to have any impact on the initial stages of NE assembly, while depletion of lamin B receptor (LBR) inhibited membrane vesicles from binding to chromosomes (Collas et al., 1996). In Xenopus egg extracts, physical and functional depletion of lamin B3 did not block NE assembly either (Newport et al., 1990; Meier et al., 1991). Finally, physical depletion of B-type lamins in turkey erythrocytes extracts had a minor effect on the chromosome-membrane vesicles binding

whereas again physical depletion of LBR completely inhibited binding (Pyrpasopoulou et al., 1996).

Lamina flexibility is required for growth of the NE and for nuclear volume increase during the cell cycle while it also influences nuclear shape. Progression into S-phase depends on the acquisition of a minimal nuclear volume (Yang et al., 1997b). Experimental data suggests that sperm-specific lamin B3 may play an important role in the organization of the meiotic cell's nuclear architecture since its expression results in the formation of hook-shaped nuclei (Furukawa and Hotta, 1993; Furukawa et al., 1994). In addition, although immunodepletion of soluble lamin B3 (>95% of total lamin B3 content) in Xenopus egg extracts does not prevent NE assembly, the nuclei formed are significantly smaller and more fragile than normal ones (Newport et al., 1990; Jenkins et al., 1993). Similar results were also obtained after addition of dominant negative lamin mutant proteins which prevent lamina filament assembly to Xenopus egg extracts (Spaun et al., 1996; Ellis et al., 1997).

In vivo, lamin filaments are closely associated with chromatin fibers (Belmont et al., 1993) and in vitro they are shown to bind interphase chromatin (Ulitzur et al., 1997; Goldberg et al., 1999a), mitotic chromosomes (Glass et al., 1993) or specific DNA sequences (Zhao et al., 1996). The binding site of vertebrate lamins to chromatin is localized at the tail domain of the proteins and it has been shown to be displaced with the core histones H2A and H2B (Goldberg et al., 1999a). As was mentioned above, the expression of A-type lamins appears to be linked to differentiation. What is more, pluripotent cells treated so as to induce differentiation can be induced to express A-type lamins (Lebel et al., 1987) and in some cases, ectopic expression of lamin A has been shown to promote differentiation (Lourim and Lin, 1992). This has lead to the suggestion that A-type lamins may be involved in differential gene expression either by anchoring

chromatin to the NE or by sequestering inhibitors (Nigg, 1989). Consistent with this suggestion is the observation that lamin A has a higher affinity for chromatin binding than B-type lamins (Höger et al., 1991), and that A-type lamins also bind the negative growth regulator $p110^{RB}$ (Ozaki et al., 1994). The effect of lamins on chromatin organization is also demonstrated in the experiments with lamin A/C null mice where the heterochromatin layer underlying the NE is either thin or absent. That suggests that lamin A/C null nuclei have difficulty attaching heterochromatin to the envelope or stabilizing its structure.

Lamin Interactions

Further understanding of the role of the lamins and lamina can be achieved through investigations of lamin binding partners. There are strong experimental evidence which show that the nuclear lamina and the INM associate through interactions between several integral nuclear membrane proteins (LBR, LAP1 and 2), and lamins. LBR has an N-terminal nucleoplasmic domain and a C-terminal region with 8 transmembrane domains. The nucleoplasmic domain of the receptor interacts with the B-type lamins (Worman et al., 1998), with HP1 (Human chromatin associate protein), and with chromatin in vitro (Ye et al., 1997). LAP1s (Lap1α, LAP1β, and LAP1γ) interact with both A- and B-type lamins (Ye and Worman, 1994). LAP2s (LAP2α, β, and γ) on the other hand associate only with lamin B1 as well as with chromatin in vitro (Foisner and Gerace, 1993; reviewed in Vaughan et al., 2000b). An exception to that is LAP2α protein which has been shown to also interact with lamin A (Dechat et al., 2000).

Lately it has been suggested that a complex similar to LAP2-lamin B1 which may be related in function to it, is formed between emerin and lamin A (Manilal et al., 1999; Morris and Manilal, 1999). In support of the above, experiments have shown that the distribution of emerin in different cell types is similar to that of lamin A and different from that of lamin B1 and B2 (Manilal et al., 1999). In addition to that, it has also been found

that lamin A binds directly to the Tsuchiya-Ostlund sequence (Ostlund et al., 1999; Tsuchiya et al., 1999) of emerin (Clements et al, 2000).

Interactions between these proteins are regulated by phoshphorylation/dephosphorylation processes. LAP2, LBR and possibly LAP1 are shown to interact with chromatin during early anaphase and are therefore believed to be involved in the nuclear lamina assembly and chromatin decondensation (reviewed in Vaughan et al., 2000b). In addition to that, LAP2β, LBR and B-type lamin are probably involved in nuclear growth during interphase (Yang et al, 1997a and 1997b; reviewed in Vaughan et al, 2000b). Finally, B-type lamins colocalize with DNA replication centers in mid S-phase (Moir et al., 1994), which suggests that they are indirectly involved in DNA replication processes (Ellis et al., 1997; reviewed in Vaughan et al, 2000b).

Absence of or mutations in emerin or lamin A/C, have been shown to give rise to the EDMD syndrome with most affected tissues being the cardiac and skeletal muscle. The most probable explanation that has been proposed for this is that these proteins are part of a nucleoskeletal network which maintains the NE integrity and protect it from mechanical stresses (Tsuchiya et al., 1999). Skeletal and cardiac muscles, in contrast to all the other cell types, are continuously subjected to mechanical stresses and that makes the effects of the absence/mutations of emerin, and lamins A and C, more severe in these tissues.

An understanding of the lamina and emerin structure, function and interactions with the INM proteins is essential for further understanding of the mechanisms underlying the EDMD syndrome, as well as other lamin associated diseases.

In the experiments conducted in this project the following were investigated:

a) the way in which mutations of lamins/emerin affect the fragility of the nuclear envelope of cells by looking at the distribution of other lamins/emerin in these cells and comparing it with control cell lines, and

b) whether or not lamins/emerin are involved in cell cycle control and growth of cells by investigating the distribution of cells in the different phases of the cell cycle, both in normal and in lamin/emerin-mutated cell lines.

Chapter 1. Lymphoblasts and fibroblasts as tools for diagnostic tests

Introduction

Emerin and lamins are present in many different cell types. However, the clinical characteristics of patients with X-linked and AD-EDMD are specific and restricted (cardiac conduction defects, early contractures at the neck, ankles and elbows, and slowly-progressive wasting of certain specific muscles), with the cardiac and skeletal muscle being particularly sensitive to lack of emerin and lamin A/C (Emery, 2000).

Staining of emerin and lamins with antibodies, as well as subcellular fractionation experiments have shown that these proteins are present in most tissues of the body and are localized mainly at the INM and lamina respectively in normal muscle cells and other tissues. Over-expressed recombinant emerin has also been reported to be present in small amounts in the cytoplasm and the plasma membrane of cultured cells (Ostlund et al., 1999), but there is no evidence as yet that it functions outside the nucleus under normal circumstances. In addition, missense mutations in the N-terminal domain of emerin causes its mislocalization either to the cytoplasm or to the nucleoplasm (Ellis et al., 1999). Apart from being the major components of the nuclear lamina, lamins also form intranuclear structures as well as transnuclear tube-like structures (Bridges et al., 1993; Moir et al., 1994; Fricker et al., 1997) in normal cells.

Although cardiac and skeletal muscle are the only tissues affected in EDMD, the pattern of expression and cell distribution of emerin and lamins is the same in all tissues. The importance of that is that the diagnosis of the syndrome at present depends on mutation analysis. Diagnosing the condition therefore could be achieved by looking at altered expression of emerin or lamins in any kind of tissue, both affected and non-affected. Cardiac and skeletal muscle is difficult to be isolated. The most common technique used

currently for the diagnosis of muscular dystrophies in muscle biopsy. Muscle biopsy is a surgical procedure in which one or more small pieces of muscle tissue are removed for microscopic or biochemical analysis. The procedure is considered minor surgery and is usually performed under local anaesthetic. It involves 2-3 inch incision, which is then closed with stitches and may feel sore for a few days. Blood and skin are alternative sources of cells that could be used in diagnostic tests. Fibroblasts can be isolated by skin biopsy, a minor procedure without serious complications, much easier and more convenient for the patient; no stitches, no scarring, no pain. Lymphoblasts are even easier to isolate. Obtaining a blood sample is rapid and easy and gives much of the same information as muscle and skin cells.

A simple test for diagnosing the condition therefore would be detecting the absence or presence of proteins and their distribution in the cell, in fibroblasts and lymphoblasts, using immunocytochemistry. This technique may be applied to suspected EDMD patients, especially sporadic, and also suspected carriers as simple and convenient.

In the first two sets of experiments we investigated the endogenous and exogenous distribution of emerin and lamins in lymphoblasts and fibroblasts, by using antibodies against these proteins and GFP-, DsRed-tagged fusion proteins (GFP-emerin, GFP-lamin A, and DsRed-lamin C). Lymphoblasts were used in these experiments as, since they are easy to be isolated, a sample for every patient in Europe is available. However, fibroblasts are more representative and easier to be used for transfections. The experiments were performed in order to assess whether or not and the extend to which lymphoblasts and fibroblasts would be appropriate for use in diagnostic tests.

Materials &Methods

Immunocytochemistry of LCLs

Cell lines and Cell culture

The lymphoblastoid cell lines from EDMD patients used in these experiments were obtained from Dr Manfred Wehnert, University of Greifswald, Germany. They were grown in 50ml flasks in 10ml RPMI1640 medium (Gibco BRL) supplemented with 10% fetal calf serum (FCS, Sigma), 2mM L-Glutamine (Gibco BRL), 100mM BME non-essential amino acid solution (Gibco BRL), and two antibiotics, 10U/ml penicillin and 100μg/ml streptomycin (Gibco BRL). Cell cultures were maintained in an incubator in humidified atmosphere with 5% CO_2 at 37°C, and the medium was replaced every three days.

Eighteen cell lines from EDMD patients and two controls were examined in total. Out of the eighteen EDMD cell lines, two were of patients with lamin A/C gene mutations (AD-1, AD-2), six of patients with emerin gene mutations (X-1, X-2, X-3, X-4, X-5, X-6), and ten of patients screened for lamin B1, LAP2β and other proteins (S-1, S-2, S-3, S-4, S-5, S-6, S-7, S-8, S-9, S-10). The mutations of these cell lines are detailed in Table 3. The two cell lines used as controls were cells of a Birkitts lymphoma cell line that does not express lamin A, and normal lymphoblastoid cells (control LCL).

Antibodies

The following primary monoclonal or polyclonal antibodies were used in these experiments: (i) RaLC against lamin C at a dilution of 1:100, (ii) Jol2 against lamin A/C

Table 3. Lymphoblastoid cell lines and mutations

Patient	Mutation
AD-EDMD	
AD-1	Exon 9, TGG>TCG;W520S
AD-2	Exon 9, ACG>AAG;T528K
X-linked EDMD	
X-1	delggcttagcaacagcgcagtgtc, nt –19 to –40 of the emerin gene promoter
X-2	del AG, nt 620-621 frameshift, stop after aa 90
X-3	Del TCTAC, nt 631-635 frameshift, stop after aa 90
X-4	ins A, nt 895; frameshift, stop after aa 126
X-5	nt 1713, C->T, codon 219, CAG->TAG, stop at codon 219
X-6	Ins TGGGC, NT 1713, stop at codon 238, (Klauck et al., 1995)
Patient	Inheritance
Sporadic EDMD	
S-1	EMD (two brothers)
S-2	EMD (two brothers)
S-3	ADEMD
S-4	EMD sporadic
S-5	EMD sporadic

S-6	EMD sporadic
S-7	EMD (two brothers)
S-8	EMD sporadic
S-9	EMD sporadic
S-10	EMD sporadic

used undiluted, (iii) GalB1 against lamin B1 at a dilution of 1:100, (iv) LN43 specific for lamin B2 at a dilution of 1:10, and (v) NCL-emerin antibody at a dilution of 1:50. All primary antibodies used in this study are listed in Table 4.

All the secondary antibodies used were obtained commercially from Jackson Immunoresearch, West Grove, P.A., and include : (i) TRITC-conjugated goat anti-rabbit IgG, (ii) TRITC-conjugated donkey anti-mouse IgG, and (iii) TRITC-conjugated donkey anti-goat IgG. All were used at a dilution of 1:50.

Dilutions for both primary and secondary antibodies were done in blocking buffer (PBS containing 1% newborn calf serum).

Immunofluorescence Microscopy

For immunofluorescence, lymphoblasts were grown in 25ml flasks and in 10ml medium, until clamps of cells were visible (growth rate varied amongst cell lines). They were then centrifuged at 1000rpm for 5min and resuspended in 3ml medium. Cells were transferred on coverslips by cytospinning at 300rpm and at low acceleration for 5min, in a cytospin III (Shandon). 10 coverslips for each cell line were prepared, two for each of the primary antibodies, and 0.250ml of cell suspension were loaded in each cytofunnel. Once on coverslips, cells were fixed in pre-chilled methanol/acetone (1:1, v/v) for 10 minutes at 4°C and washed three times in PBS. Before primary antibody addition, coverslips were washed with blocking buffer for 30 seconds. Antibody incubation time was 1 hr at room temperature for both primary and secondary antibodies, followed by three 15min washes with blocking buffer after the primary antibody addition and three 15min washes with PBS after the secondary antibody addition. Coverslips were mounted face down in Mowiol (Calbiochem) containing 1μg/ml DAPI (4', 6-diamidin-2-phenylinolol-dihydrochloride) and 1μg/ml DABCO (1,4-diazabicyclol [2.2.2]octane).

Table 4. Types of primary antibodies used

Antibody	Protein target	Antibody type	Dilution	Source
Ral C	Lamin C	Rabbit-polyclonal	1:100	Venables et al., 2001
Jol 2	Lamin A/C	Mouse-monoclonal	Undiluted	Dyer et al., 1999
Gal B1	Lamin B1	Goat-polyclonal	1:100	Santa Cruz
LN43	Lamin B2	Mouse-monoclonal	1:100	Dyer et al., 1999
NCL-emerin	Emerin	Mouse-monoclonal	1:50	NovaCastra

Immunofluorescence samples were viewed with a Zeiss Axiovert 10 microscope equipped for epifluorescence using a plan-APOCHROMAT 63x/1, 40 oil immersion lens. Images were captured with a 12-bit CCD camera using IPLab Scientific Imaging Software (Scanalytis).

Cell counting was conducted manually. More specifically, microscopic fields were randomly selected from each slide and were first viewed with the DAPI filter. All healthy looking single nuclei were counted, while clusters of cells with overlapping nuclei were not included in the scoring. The filter was then switched to Rhodamine and the cellular distribution of lamins and emerin in those nuclei was recorded as rim, cytoplasm, aggregates, and absent. 100 cells were counted from each of the two slides prepared per primary antibody, thus, 200 cells were counted in total.

Immunocytochemistry of fibroblasts

Cell lines and Cell culture

Skin fibroblasts from EDMD patients were supplied by Professor Irena Housmanowa, Neurology Centre, Warsaw. They were grown in DMEM medium (Gibco BRL) supplemented with 10% fetal calf serum (Sigma), 10U/ml penicillin and 100μg/ml streptomycin (Gibco BRL), in 90mm petri dishes. Cell cultures were maintained in an incubator at a humidified atmosphere, with 5% CO_2 at 37°C and the cells were passaged at confluence for maintenance.

Five fibroblastic cell lines were examined in total (four from patients and one control) after being transfected with pEGFP-LA, pEGFP-Emerin and DSRed1-LC constructs. The EDMD cell lines were from: an emerin null patient (X-EDMD1), that

Table 5. Fibroblastic cell lines and mutations

Patient	Mutation	Emerin expression	Lamin A/C expression
X-EDMD1	386 del C	-ve	+ve
X-EDMD2	A111G	-ve	+ve
X-EDMD Carrier	386 del C	-ve and +ve	+ve
AD-EDMD	C1357T	+ve	+ve

patient's mother who is a manifested carrier (X-EDMD Carrier), a patient with an emerin gene mutation (X-EDMD2), and an autosomal dominant EDMD patient (AD-EDMD). Details of the mutations of the cell lines examined are shown in Table 5.

Plasmid Construction

Green Fluorescent Protein (GFP) Fusion: To make pEGFP-LA, the pEGFP vector (Clontech Laboratories, Inc.) was cut with EcoRI and BamHI restriction enzymes and was thus linearized. Lamin A gene was cut out from pEGM-LA plasmid with the same enzymes, EcoRI and BamHI, and was subcloned in the linear pEGFP to construct pEGFP-LA fusion protein. pEGFP-emerin was constructed previously (Vaughan et al., 2001).

Red Fluorescent Protein (DsRed) Fusion: To make DsRed1-LC fusion protein, lamin C gene was amplified from a pET7-LC plasmid using the primers 5'-CTGAGAATTCAATGGAGACCCCGTCC-3' (forward primer) and 5'-TATATAGGTACCGCGGCGGCTACCACT-3' (reverse primer), ordered from MWG-Biotech AG. The primers were designed so as to contain an EcoRI restriction site and a KpnI restriction site in the forward and reverse primer respectively. The PCR product was digested with EcoRI and KpnI restriction enzymes. The DsRed1 plasmid (Clontech Laboratories, Inc.) was also cut with the same enzymes. The two linear DNAs, lamin C and DsRed, were then ligated through their cut ends to construct DsRed1-LC.

Transfections and Microscopy

Fibroblasts were transfected using a multiporator for eukaryotic cells (Eppendorf AG, Cambridge). For transfection, cells were harvested by trypsinization at 70-80% confluency and centrifuged at 1000rpm for 10 min at room temperature. They were then resuspended in DMEM containing 0.5% FCS and their number was determined. Cells were

centrifuged again under the same conditions as before, and were resuspended in hypoosmolar electroporation buffer at a concentration of 10^6cells/ml. Plasmid DNA at a final concentration of 10μg/ml was added to the cell suspension, and 400μl of this mixture was transferred into the electroporation cuvette (2mm gap width aluminum cuvette). Electroporation conditions were as follows: mode: eukaryotes, voltage: 400V, time: 100μsec, no of pulses: 1. After the pulse was delivered, the cell suspension was allowed to stand in the cuvette for 10min at room temperature before being transferred to a 45mm culture dish containing 3ml medium and coverslips. The dish was kept in an incubator with 5% CO_2, at 37°C. 36hrs after transfection, the coverslips were removed from the dishes, were washed with PBS and were fixed with methanol/acetone (1:1, v/v) for 10min at 4°C. They were then washed with PBS again, mounted on slides and observed under a microscope as described previously.

Results

Immunocytochemistry of LCLs

The normal cellular distribution of lamin proteins and emerin is repeatedly shown by a number of studies to be affected in muscle cells taken from patients with EDMD. Here we investigated the distribution of endogenous lamin A, C, B1, B2 and emerin in lymphoblasts (LCLs) of patients with X-linked, autosomal dominant and sporadic EDMD using immunofluorescence microscopy. The results obtained were compared with those collected from two lymphoblastoid cell lines used as controls.

Lamin and emerin distribution in LCLs of patients with autosomal dominant EDMD.

Immunofluorescence on LCLs taken from two AD-EDMD patients stained with antibodies against lamin A, C, B1, B2 and emerin, gave consistent results for both cell lines examined. Table 6 summarizes the immunofluorescence data collected from these two patients.

From Table 6 and Figure 2 it can be seen that in these cell lines, lamin C was localized in the nuclear rim and in structures inside the nucleus giving a very bright staining. Lamins A, B1 and B2 were mainly found in the nuclear rim. In a significant proportion of cells however cytoplasmic staining was also observed with these antibodies showing translocation of these proteins from the rim to the cytoplasm. The same holds for emerin as well. Emerin was shown to be localized in the nuclear rim in most cells but cytoplasmic staining was also observed in some of the cells scored. In both cell lines and with all antibodies' staining only a few cells remained unstained while no cells or just a few in the case of lamin A in AD-1 and lamin C in AD-2 patient, showed aggregates of the protein.

Table 6. Lymphoblast staining of patients with AD-EDMD.

(The numbers in the table show the number of nuclei with the particular staining pattern out of the total 200 counted per antibody)

	STAINING				
Patient : AD-1	RIM		CYTOPLASM	AGGREGATES	ABSENT
	Bright	Dull			
Lamin C	117	64	6	0	13
Lamin A/C	64	73	43	10	10
Lamin B1	93	28	78	0	1
Lamin B2	88	59	36	0	17
Emerin	63	111	21	0	5

	STAINING				
Patient : AD-2	RIM		CYTOPLASM	AGGREGATES	ABSENT
	Bright	Dull			
Lamin C	142	41	7	3	7
Lamin A/C	140	22	36	0	2
Lamin B1	20	100	45	0	35
Lamin B2	145	22	24	0	9
Emerin	59	99	42	0	0

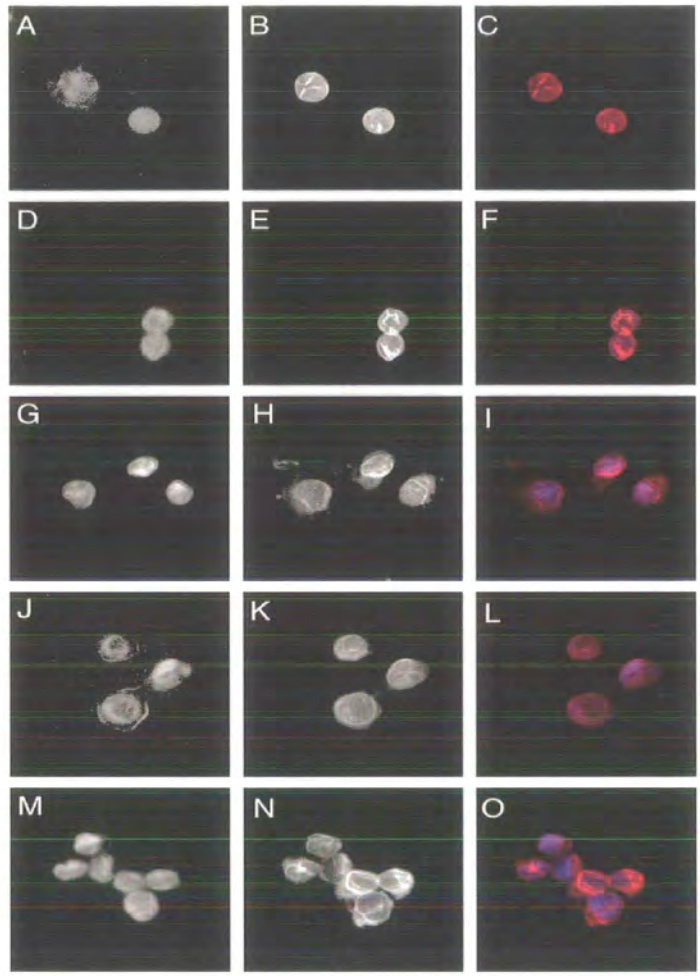

Fig.2. The distribution of lamin C, lamin A/C, lamin B1, lamin B2 and emerin in lymphoblastoid cell lines of AD-EDMD. The distribution of DNA was detected with DAPI (panels A, D, G, J, M). The distribution of lamin C, lamin A/C, lamin B1, lamin B2, and emerin, is shown in black and white micrographs in panels B, E, H, K, and N respectively. Two colour merged images in which DAPI is shown in blue and the protein stained in red are shown in panels C, F, I, L, O.

Lamin and emerin distribution in LCLs of patients with X-linked EDMD.

Immunofluorescence data collected from the five X-EDMD patients' cell lines is summarized in Table 7 and displayed in Figure 3. In all cell lines of this group of patients emerin staining was as expected absent, with the exception of X-1 patient. X-1 was known to have quantitatively less emerin present in muscle cells compared to normal individuals. Emerin staining in this patient's LCLs was visible in the nuclear rim as well as in structures inside the nucleus, but the staining was very dull. In addition, some cells appeared to have cytoplasmic staining of emerin as well. Lamin C was shown to be slightly affected in all five cell lines examined. Staining in this case was seen only in the rim and in internal structures and not in the cytoplasm. However, in a small proportion of cells lamin C staining was absent. Finally, in all cell lines cytoplasmic translocation was observed for at least one or more lamins without however any evident pattern. More specifically, in patients X-1 and X-4, lamin A, lamin B1, and lamin B2 was translocated to the cytoplasm in a small but significant proportion of cells scored. In patients X-2, X-3, and X-5, lamin A and lamin B1 was seen in the cytoplasm in some cells, while there was no cytoplasmic staining for lamin B2 in these patients. Finally, patient X-6 showed translocation to the cytoplasm only in the case of lamin B1. All other lamins in this patient (lamin A, C, and B2) were clearly and only seen at the nuclear rim.

Lamin and emerin distribution in LCLs of EDMD patients screened for lamin B1, LAP2beta and other proteins.

Data collected from the staining of the cell lines of the sporadic EDMD patients is shown in Table 8 and in Figure 4. Results in this group of patients varied significantly amongst the cell lines examined. No general pattern of change of distribution could therefore be seen. Interestingly however, in four out of the ten cell lines examined, there was either a dull staining of emerin throughout the whole nucleus (S-1, S-2), or no staining

Table 7. Lymphoblast staining of patients with X-linked EDMD

(The numbers in the table show the number of nuclei with the particular staining pattern out of the total 200 counted per antibody)

	STAINING				
Patient : X-1	RIM		CYTOPLASM	AGGREGATES	ABSENT
	Bright	Dull			
Lamin C	83	111	0	0	6
Lamin A/C	92	88	11	0	9
Lamin B1	20	120	50	0	10
Lamin B2	40	145	11	0	4
Emerin	10	160	25	0	5

	STAINING				
Patient : X-2	RIM		CYTOPLASM	AGGREGATES	ABSENT
	Bright	Dull			
Lamin C	132	58	4	0	6
Lamin A/C	157	22	15	3	3
Lamin B1	36	154	5	0	5
Lamin B2	85	102	0	8	5
Emerin	0	0	0	0	200

	STAINING				
Patient : X-3	RIM Bright	RIM Dull	CYTOPLASM	AGGREGATES	ABSENT
Lamin C	114	71	3	0	12
Lamin A/C	106	71	14	0	9
Lamin B1	23	155	15	0	7
Lamin B2	42	150	5	0	3
Emerin	0	0	0	0	200

	STAINING				
Patient : X-4	RIM Bright	RIM Dull	CYTOPLASM	AGGREGATES	ABSENT
Lamin C	121	61	0	2	16
Lamin A/C	118	45	16	4	17
Lamin B1	91	80	11	0	18
Lamin B2	140	45	15	0	0
Emerin	0	0	0	0	200

	STAINING				
Patient : X-5	RIM Bright	Dull	CYTOPLASM	AGGREGATES	ABSENT
Lamin C	150	42	2	0	6
Lamin A/C	143	43	10	2	2
Lamin B1	47	140	7	0	6
Lamin B2	65	128	0	2	5
Emerin	0	0	0	0	200

	STAINING				
Patient : X-6	RIM Bright	Dull	CYTOPLASM	AGGREGATES	ABSENT
Lamin C	100	70	0	0	30
Lamin A/C	109	79	0	0	12
Lamin B1	20	127	33	0	20
Lamin B2	32	163	0	0	5
Emerin	0	0	0	0	200

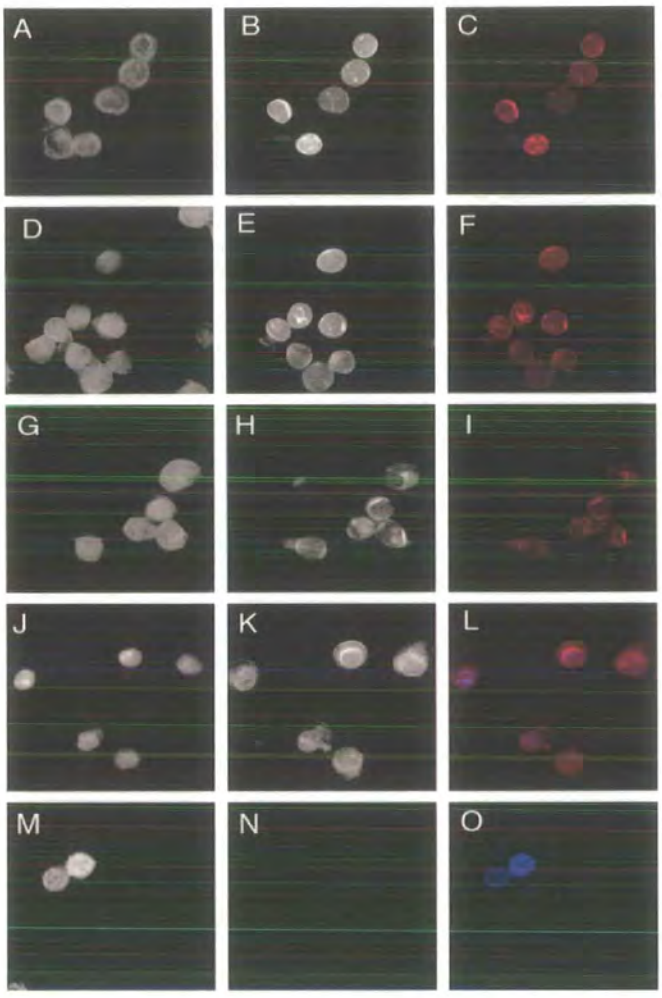

Fig.3. The distribution of lamin C, lamin A/C, lamin B1, lamin B2 and emerin in lymphoblastoid cell lines of X-EDMD patients. The distribution of DNA was detected with DAPI (panels A, D, G, J, M). The distribution of lamin C, lamin A/C, lamin B1, lamin B2, and emerin, is shown in black and white micrographs in panels B, E, H, K, and N respectively. Two colour merged images in which DAPI is shown in blue and the protein stained in red are shown in panels C, F, I, L, O.

Table 8. Lymphoblast staining of patients with sporadic EDMD

(The numbers in the table show the number of nuclei with the particular staining pattern out of the total 200 counted per antibody)

	STAINING				
Patient : S-1	RIM		CYTOPLASM	AGGREGATES	ABSENT
	Bright	Dull			
Lamin C	80	84	8	4	24
Lamin A/C	64	76	48	5	7
Lamin B1	34	84	52	0	30
Lamin B2	75	54	61	3	7
Emerin	8	4	0	0	188

	STAINING				
Patient : S-2	RIM		CYTOPLASM	AGGREGATES	ABSENT
	Bright	Dull			
Lamin C	51	71	0	0	78
Lamin A/C	92	87	3	0	18
Lamin B1	10	100	70	0	20
Lamin B2	110	50	30	0	10
Emerin	0	10	15	0	175

	STAINING				
Patient : S-3	RIM Bright	RIM Dull	CYTOPLASM	AGGREGATES	ABSENT
Lamin C	107	66	0	0	27
Lamin A/C	102	67	3	3	25
Lamin B1	48	90	54	0	8
Lamin B2	63	68	61	3	5
Emerin	52	80	65	0	3

	STAINING				
Patient : S-4	RIM Bright	RIM Dull	CYTOPLASM	AGGREGATES	ABSENT
Lamin C	110	79	0	0	11
Lamin A/C	102	87	3	0	8
Lamin B1	80	62	54	0	4
Lamin B2	91	56	46	0	7
Emerin	94	83	21	0	2

	STAINING				
Patient : S-5	RIM Bright	RIM Dull	CYTOPLASM	AGGREGATES	ABSENT
Lamin C	68	96	0	0	36
Lamin A/C	62	115	0	0	23
Lamin B1	10	160	0	0	30
Lamin B2	32	150	0	0	18
Emerin	40	155	0	0	5

	STAINING				
Patient : S-6	RIM Bright	RIM Dull	CYTOPLASM	AGGREGATES	ABSENT
Lamin C	107	80	0	6	7
Lamin A/C	86	90	2	6	16
Lamin B1	15	160	20	0	5
Lamin B2	27	148	15	0	10
Emerin	All cells stained pink				

	STAINING				
Patient : S-7	RIM Bright	Dull	CYTOPLASM	AGGREGATES	ABSENT
Lamin C	100	90	0	0	10
Lamin A/C	105	80	6	0	9
Lamin B1	81	98	18	0	3
Lamin B2	39	120	31	0	10
Emerin	70	102	24	0	4

	STAINING				
Patient : S-8	RIM Bright	Dull	CYTOPLASM	AGGREGATES	ABSENT
Lamin C	77	99	3	0	21
Lamin A/C	106	70	17	0	7
Lamin B1	20	137	40	0	3
Lamin B2	57	116	22	0	5
Emerin	10	173	10	0	7

	STAINING				
Patient : S-9	RIM Bright	RIM Dull	CYTOPLASM	AGGREGATES	ABSENT
Lamin C	109	52	8	5	26
Lamin A/C	77	74	26	9	14
Lamin B1	65	78	28	0	29
Lamin B2	137	35	23	2	3
Emerin	36	120	17	1	26

	STAINING				
Patient : S-10	RIM Bright	RIM Dull	CYTOPLASM	AGGREGATES	ABSENT
Lamin C	145	35	2	2	16
Lamin A/C	141	40	2	2	15
Lamin B1	18	118	6	0	58
Lamin B2	92	88	4	0	16
Emerin	All cells stained pink				

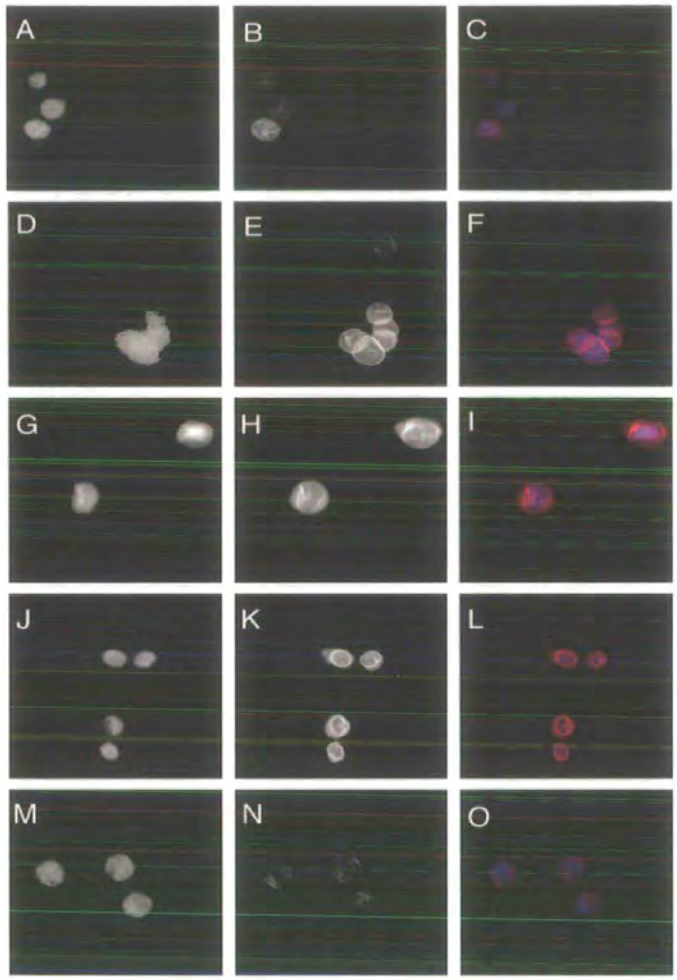

Fig.4. The distribution of lamin C, lamin A/C, lamin B1, lamin B2 and emerin in lymphoblastoid cell lines of sporadic EDMD patients The distribution of DNA was detected with DAPI (panels A, D, G, J, M). The distribution of lamin C, lamin A/C, lamin B1, lamin B2, and emerin, is shown in black and white micrographs in panels B, E, H, K, and N respectively. Two colour merged images in which DAPI is shown in blue and the protein stained in red are shown in panels C, F, I, L, O. (Images taken from S-1 patient.)

at all (S-6, S-10). Generally, in all cell lines, all lamins' staining was shown to be affected either by partial translocation to the cytoplasm or/and by absence of staining or dull staining. More specifically, in many cell lines there was no lamin C staining in a relatively high proportion of cells while interestingly, this protein was the only one that was almost never seen in the cytoplasm in any of the cell lines examined. Lamin A and lamin B1 on the other hand were seen both in the cytoplasm and/or were absent in a proportion of cells in the majority of cell lines. Lamin B2, was found to be translocated to the cytoplasm in a proportion of cells in all cell lines.

Lamin and emerin distribution in LCLs of control cells.

The immunofluorescence results of the two cell lines used as controls are shown in Table 9 and in Figure 5. Burkitts lymphoma cell line which is deficient in lamin A showed very weak staining for both lamin A and lamin C. With both antibodies' staining, the nuclei of the cells appeared homogenously stained under the microscope with no apparent rim staining. In contrast, in control LCL cell line, staining of both lamin A and C was in the nuclear rim and in structures inside the nucleus as expected. Lamins B1 and B2 as well as emerin were mostly localized in the rim and in structures inside the nucleus in both cell lines. However, a proportion of cells (higher in Burkitts lymphoma than in control LCL) stained with antibodies directed against these proteins also showed cytoplasmic staining.

The pictures of LCLs' staining with antibodies shown in the figures were taken from some of the cell lines examined and are representatives, since the staining of all the other cell lines was similar.

Table 9. Lymphoblast staining of control cells

(The numbers in the table show the number of nuclei with the particular staining pattern out of the total 200 counted per antibody)

	STAINING				
Control: Burkitts lymphoma	RIM Bright	RIM Dull	CYTOPLASM	AGGREGATES	ABSENT
Lamin C	Very dull staining				
Lamin A/C	Very dull staining				
Lamin B1	100	66	27	0	7
Lamin B2	85	79	32	0	4
Emerin	90	78	24	0	8

	STAINING				
Control: Control LCL	RIM Bright	RIM Dull	CYTOPLASM	AGGREGATES	ABSENT
Lamin C	156	44	0	0	0
Lamin A/C	147	51	2	0	0
Lamin B1	121	54	10	0	15
Lamin B2	93	97	7	0	3
Emerin	75	103	15	0	7

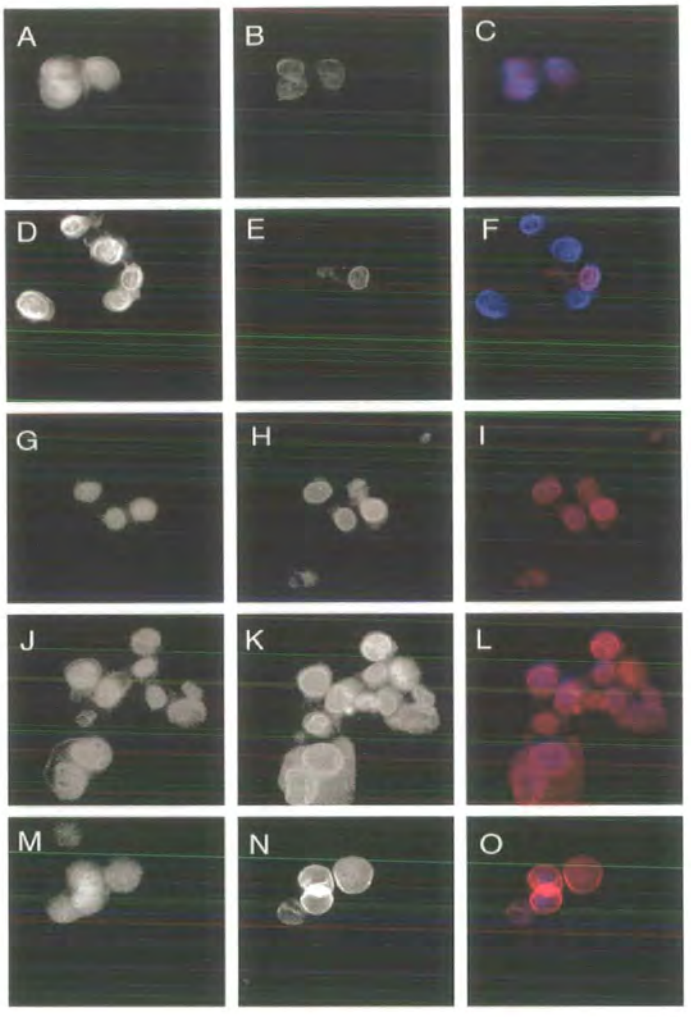

Fig.5. The distribution of lamin C, lamin A/C, lamin B1, lamin B2, and emerin in control LCL. The distribution of DNA was detected with DAPI (panels A, D, J, M). The distribution of lamin C, lamin A/C, lamin B1, lamin B2, and emerin, is shown in black and white micrographs in panels B, E, H, K, and N, respectively. Two colour merged images in which DAPI is shown in blue and the protein stained in red are shown in panels C, F, I, L, O.

Immunocytochemistry of fibroblasts

Construction of DsRed1-Lamin C

Lamin C was amplified by PCR and the product resolved on agarose gel along with positive and negative controls for the PCR reaction (Fig.6i). The band was cut, purified and subcloned into the DsRed1 vector. To verify that the cloning procedure was successful diagnostic cuts were performed with EcoRI and KpnI restriction enzymes. The cut DNA the linearized vector, and lamin C PCR product were all run on an agarose gel (Fig.6ii). The start and end parts of the sequence of the construct is shown in Figure 7.

Constructs of lamin A fused to GFP, emerin fused to GFP and lamin C fused to DsRed were created and transiently expressed in fibroblasts of EDMD patients and of healthy individuals. To investigate the cellular localization of the transiently expressed constructs, immunofluorescence microscopy was performed using fibroblasts fixed 36hrs after transfection.

Distribution of DsRed-LaminC in fibroblasts of AD-EDMD, and X-linked EDMD patients

In patient X-EDMD1 who is an emerin null patient, the GFP-emerin construct was distributed in the NE in the majority of transfected fibroblasts. However, in some fibroblasts the construct was also found translocated outside the nucleus, dispersed into the cytoplasm. In Fig.8, panels A-C, a fibroblast transfected with GFP-emerin is shown. Emerin in that fibroblast is localized in the NE with no cytoplasmic staining seen. The DsRed-LC construct was observed to be distributed in the NE and, in addition, in patch-like structures inside the nucleus. The distribution of the construct in the NE is illustrated in Fig.8, panels D-F. The patch-like structures are not visible here. Finally, the GFP-LA construct was clearly seen only in the NE and no cell was recorded in which GFP-LA was located elsewhere. The NE distribution of GFP-LA is shown in Fig.8, panels G-I.

Fig.6. Gels illustrating the production of lamin C from the PCR reaction and the diagnostic cutting of the DsRed-LC construct

(i)

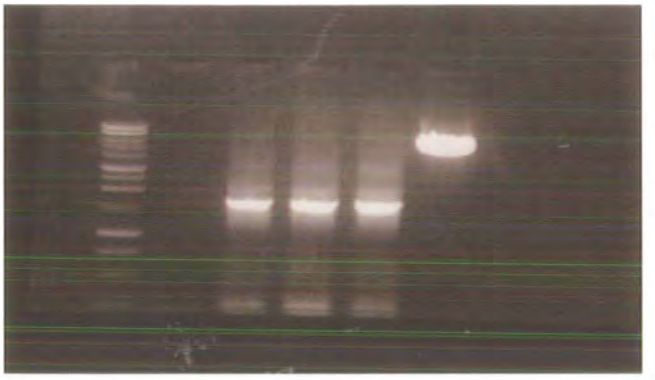

1 2 3 4 5 6

Lane 1 : Ladder

Lane 2 : Negative control

Lane 3, 4, 5 : DsRed-LC

Lane 6 : Positive control

(ii)

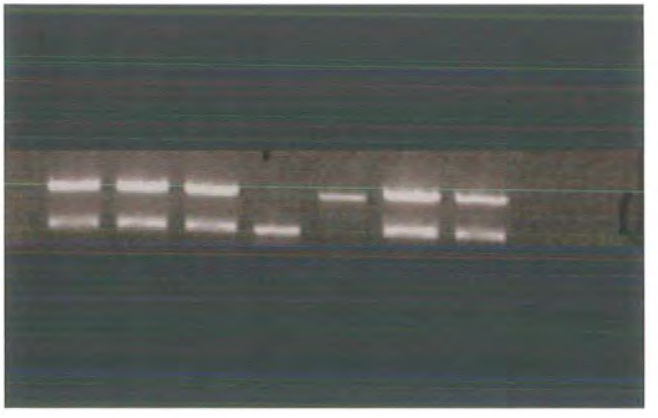

1 2 3 4 5 6 7

Lane 1, 2, 3, 6, 7 : DsRed-LC construct cut with EcoRI and KpnI

Lane 4 : Lamin C, product of PCR reaction

Lane 5 : Linear DsRed

Fig.7. The nucleotide sequence of DsRed-LC construct

Sequence from primer C

ATACNCCTCGTGGAGCAGTACGAGCGCACCGAGGGCCGCCACCACCTGTTCCTGCTCAG
ATCTCGAGCTCAAGCTTCGAATTCAATGGAGACCCCGTCCCAGCGGCGCGCCACCCGCA
GCGGGGCGCAGGCCAGCTCCACTCCGCTGTCGCCCACCCGCATCACCCGGCTGCAGGAG
AAGGAGGACCTGCAGGAGCTCAATGATCGCTTGGCGGTCTACATCGACCGTGTGCGCTC
GCTGGAAACGGAGAACGCAGGGCTGCGCCTTCGCATCACCGAGTCTGAAGAGGTGGTCA
GCCGCGAGGTGTCCGGCATCAAGGCCGCCTACGAGGCCGAGCTCGGGGATGCCCGCAA
GACCCTTGACTCAGTAGCCAAGGAGCGCGCCCGCCTGCAGCTGGAGCTGAGCAAAGTGC
GTGAGGAGTTTAAGGAGCTGAAAGCGCGCAATACCAAGAAGGAGGGTGACCTGATAGCT
GCTCAGGCTCGGCTGAAGGACCTGGAGGCTCTGCTGAACTCCAANGAGGCCGCACTGAG
CACTGNTCTTAGTGAGAAGCGCACGCTGGANGGGCGAGCTGCATGATTTGCGGGGCCCA
GGTGGNCAANCTTTGAGGCANCCCTANGTGAAGGGCCAAAAAGCAAC

Sequence from primer N

AAGNCGTCCAGGCGAAGGGCAGGGGGCCGCCCTTGGTCACCTTCAGCTTCACGGTGTTG
TGGCCCTCGTAGGGGCGGCCCTCGCCCTCGCCCTCGATCTCGAACTCGTGGCCGTTCAC
GGTGCCCTCCATGCGCACCTTGAAGCGCATGAACTCCTTGATGACGTTCTTGGAGGAGC
GCACCATGGTGGCGACCGGTAGCGCTAGCGGATCTGACGGTTCACTAAACCAGCTCTGC
TTATATAGACCTCCCACCGTACACGCCTACCGCCCATTTGCGTCAATGGGGCGGAGTTGT
TACGACATTTTGGAAAGTCCCGTTGATTTTGGTGCCAAAACAAACTCCCATTGACGTCAA
TGGGGTGGAGACTTGGAAATCCCCGTGAGTCAAACCGCTATCCACGCCCATTGATGTAC
TGCCAAAACCGCATCACCATGGTAATAGCGATGACTAATACGTAGATGTACTGCCAAGTA
GGAAAGTCCCATAAGGTCATGTACTGGGCATAATGCCAGGCGGGCCATTTACCGTCATT
GACGTCAATAGGGGGCGTACTTGGCATATGATACACTTGATGTACTGCCAAGTGGGCAG
TTTACCGTAAATACTCCACCCATTGACGTCAATGGAAAGTCCTATTGGNGTTACTATGGG
AACATACNTCATTATTGACNTNAATG

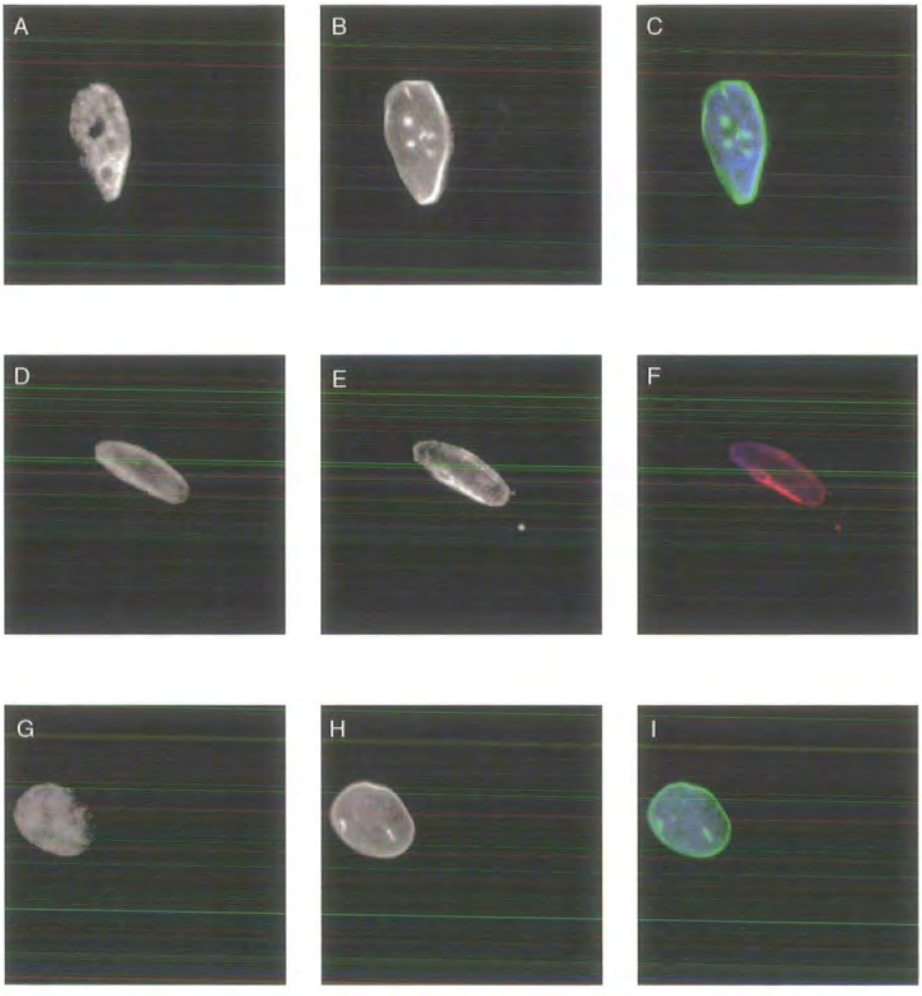

Fig.8. The distribution of GFP- emerin (A-C), DsRed-lamin C (D-F) and GFP-lamin A (G-I) in X-EDMD1 patient's fibroblasts. Panels A, D and G show DAPI staining. Panels B, E, and H show staining with GFP-emerin, DsRed-lamin C and GFP-lamin A respectively and panels C, F, and I are merged images.

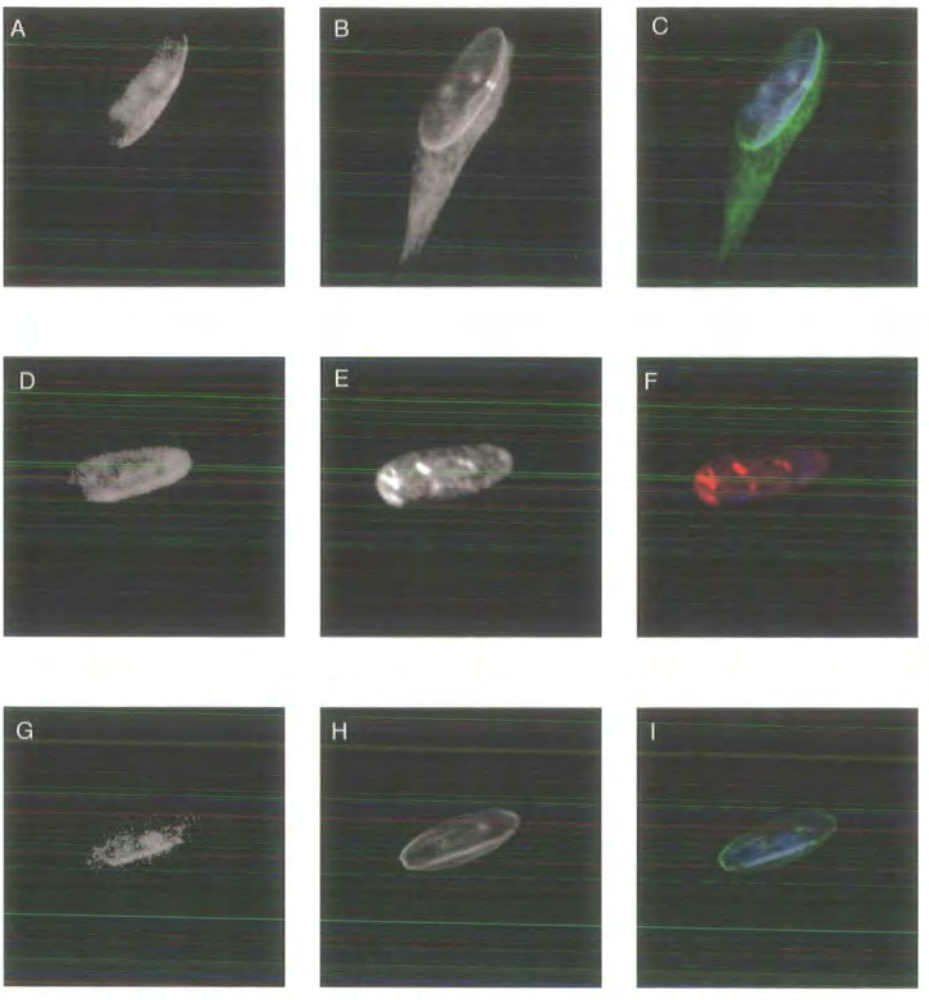

Fig.9. The distribution of GFP- emerin (A-C), DsRed-lamin C (D-F) and GFP-lamin A (G-I) in X-EDMD patient's fibroblasts. Panels A, D and G show DAPI staining. Panels B, E, and H show staining with GFP-emerin, DsRed-lamin C and GFP-lamin A respectively and panels C, F, and I are merged images.

The same pattern of distribution was also observed with all constructs in the case of X-EDMD Carrier, who is emerin null only in half of the cells, as shown in Fig.9. The GFP-emerin construct illustrated in panels A-C is shown here to be partly distributed in the NE and partly dispersed into the cytoplasm. The DsRed-LC construct in panels D-F is an example of a fibroblast manifesting patch-like structures inside the nucleus with no NE distribution. In panels G-I, GFP-LA construct is again seen in the NE.

In patient X-EDMD2 who is emerin deficient, GFP-emerin construct was mainly found in the cytoplasm, while in some cells it could also be seen in the NE. A fibroblast with cytoplasmic distribution of GFP-emerin as well as some NE localization of the construct is illustrated in Fig.10, panels A-C. In this patient, DsRed-LC was found both in structures (patches) inside the nucleus and in the NE as seen in panels D-F. Finally, GFP-LA was again only seen in the NE, panels G-I

In AD-EDMD, a patient with lamin A/C gene mutation, GFP-emerin construct was seen both in the NE and dispersed into the cytoplasm. In Fig.11, panels A-C, a fibroblast with mainly cytoplasmic localization of GFP-emerin is shown. The DsRed-LC construct was found distributed in the NE and in patches inside the nucleus, as seen in panels D-F. On the other hand however, AD-EDMD fibroblasts transfected with GFP-LA showed NE distribution in only very few cells, which was in addition dull. A representative cell transfected with the GFP-LA construct is shown in panesl G-I.

Normal fibroblasts were transfected with all the created constructs and the results obtained were compared to those of the EDMD cell lines. The GFP-LA construct was found in the NE and the DsRed-LC one was seen both in the NE and inside the nucleus forming aggregates. The GFP-emerin construct on the other hand was seen in the NE as well as in the cytoplasm. Results of normal fibroblasts transfected with the three constructs are not shown here.

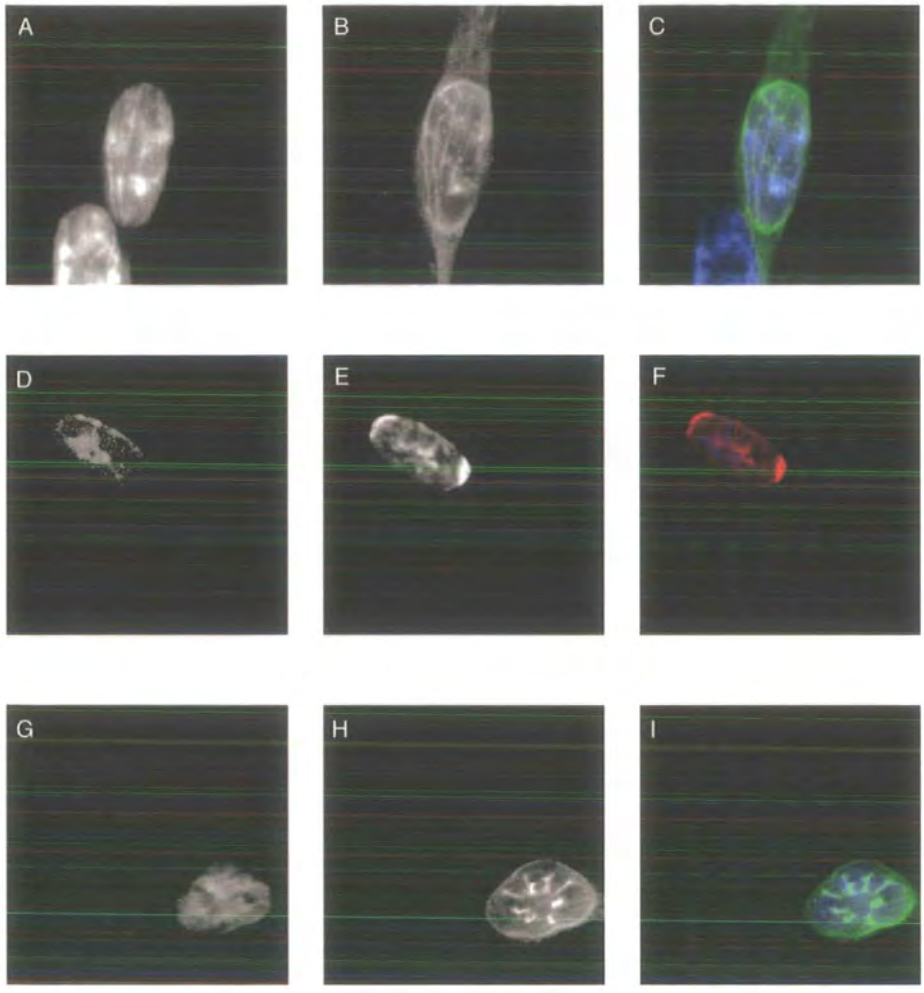

Fig.10. The distribution of GFP- emerin (A-C), DsRed-lamin C (D-F) and GFP-lamin A (G-I) in X-EDMD2 patient's fibroblasts. Panels A, D and G show DAPI staining. Panels B, E, and H show staining with GFP-emerin, DsRed-lamin C and GFP-lamin A respectively and panels C, F, and I are merged images.

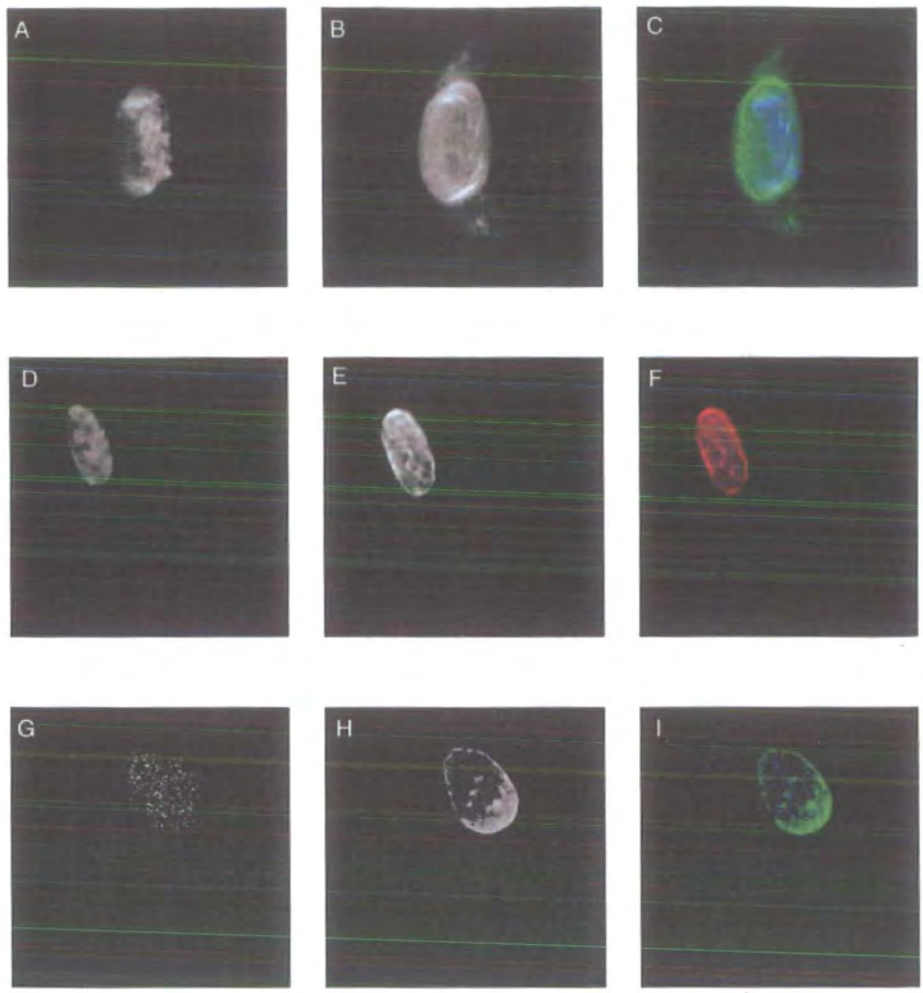

Fig.11. The distribution of GFP- emerin (A-C), DsRed-lamin C (D-F) and GFP-lamin A (G-I) constructs in AD-EDMD patient's fibroblasts. Panels A, D and G show DAPI staining. Panels B, E, and H show staining with GFP-emerin, DsRed-lamin C and GFP-lamin A respectively and panels C, F, and I are merged images.

Chapter 2. The nuclear lamina and cell cycle effects in EDMD cells

Introduction

In recent years it has become evident that a number of human genetic diseases arise as a result of mutations in proteins that are involved in the establishment of nuclear structure and architecture (Wilson, 2000; Hutchison et al., 2001). This indicates that nuclear architecture is closely related to and is very important for nuclear function.

Both emerin and lamins as mentioned in the general introduction are implicated directly or indirectly in the organization and maintenance of the nuclear structure, as well as in nuclear function. Mutated emerin gives rise to EDMD implying a possible function in transcription regulation (Morris and Manilal, 1999). In addition, lamins have been repeatedly reported to be involved in DNA replication (Ellis et al., 1997; Spann et al., 1997; Moir et al., 2000). The above findings suggest that these proteins may be further involved in the regulation of the cell cycle and the progression of the cells through it.

The measurement of the DNA content of cells was one of the first major applications of flow cytometry. The DNA content of a cell can provide a great deal of information on the distribution of cells at the different phases of the cell cycle, and consequently on the effect of a number of factors including mutated or absent proteins on the cell cycle.

In this set of experiments we investigated the effects of mutated or absent emerin and mutated lamin A/C on cell cycle progression in fibroblasts from EDMD patients using flow cytometry. Fibroblasts from a normal individual were also used for comparison. Since emerin's and lamins' role-function in the cell imply that they also affect indirectly the progression of the cells through the cell cycle, it was expected that the distribution of cells around the cycle would be altered in fibroblasts from patients. Normal fibroblasts display

regulated cell growth and division in culture and they respond to high density in culture by entering the G0 phase of the cycle. In the mutant cell lines examined, two possible types of abnormalities were expected; an abnormal progression through S-phase (longer S-phase) and an abnormal response to growth signals (G2 accumulation instead of G0 at confluency).

Materials and Methods

Cell lines and Cell culture

The same cell lines of skin fibroblasts from EDMD patients and the same culture conditions were used in this study as described in chapter 1. Normal fibroblasts were also used in these experiments. Five fibroblastic cell lines were examined in total (four from patients and one from a healthy individual-control). More specifically, the EDMD cell lines were from: an emerin null patient (X-EDMD1), that patient's mother who is a manifested carrier (X-EDMD Carrier), a patient with an emerin gene mutation (X-EDMD2), and an autosomal dominant EDMD patient (AD-EDMD). Details of the mutations of the cell lines examined are shown in Table 5.

Skin fibroblasts from EDMD patients were supplied by Professor Irena Housmakowa, Neurology Centre, Warsaw. They were grown in DMEM medium (Gibco BRL) supplemented with 10% fetal calf serum (Sigma), 10U/ml penicillin and 100μg/ml streptomycin (Gibco BRL), in 90mm petri dishes. Cell cultures were maintained in an incubator at a humidified atmosphere, with 5% CO_2 at 37°C and the cells were passaged at confluence for maintenance.

DNA staining and FACS analysis

For FACS analysis cells were grown in 90mm petri dishes, allowed to reach confluency, and subcultured at a dilution of 1:3. Fibroblasts were analyzed on day 3, 5, and 10 after passage. The DNA of the fibroblasts was stained using propidium iodide. Cells from each of the five cell lines were harvested by trypsinization on day 3, 5 and 10 after subculturing and were collected by centrifugation at 1000rpm for 5min. They were then resuspended in 1ml PBS and centrifuged again at 2000rpm for 5min. After that, they were

resuspended in and fixed with 0.5ml pre-chilled 70% ethanol while vortexing. After being kept for 10 minutes at 4°C, the fixed cells were centrifuged at 2000rpm for 5min and washed twice in PBS. Finally, they were treated with 100μl ribonuclease (100μg/ml) for 5min at room temperature and stained with 400μl propidium iodide (50μg/ml). Cell cycle analysis was performed in Coulter Epics XL FACS analyzer. Flow cytometric data was acquired using System II software.

Results

One of the characteristic features of emerin is its high serine residues content which can be phosphorylated/dephosphorylated by various kinases. Studies have shown that normal emerin can occur in four different phosphorylated forms, three of which seem to be associated with the cell cycle as discussed previously. In addition, nuclear lamins have also been speculated to be involved in cell cycle progression by playing a role in NE assembly and growth. To further investigate the involvement of emerin and lamins in cell cycle progression, we performed cell cycle analysis in fibroblasts of patients with different forms of EDMD using a FACS analyzer. Representative data obtained from these experiments is shown in Fig.12 - Fig.16. The fibroblasts were tested at passage 7, 8 and 9.

In Figure 12 the distribution of the control fibroblasts throughout the cell cycle at passage 7 is shown. The general pattern was two peaks, one very sharp at the G0-G1 phase of the cycle and one much smaller and broader at G2 phase. The fraction of cells was the same at all passages and at different cell cycle phases for each day of analysis and was regarded as normal cell cycle distribution. More specifically, on day 3 (Fig. 12a) 61.6% of the cells were in G1, 15.9% were in S, and 6.33% were in G2/M (86.6% counted). On day 5 (Fig. 12b), 63.2% of the cells were in G1, 9.27% were in S, and 6.31% were in G2/M (78.1% cells counted). Finally, on day 10 (Fig. 12c), 66.5% of the cells were in G1, 12% were in S, and 4.46% were in G2/M (88.3% cells counted).

In Figure 13, data collected from X-EDMD1 patient at passage 7 and on days 3, 5 and 10, is illustrated. At passage 7, and on day 5, the distribution of cells throughout the cell cycle was as in the control, although the G0-G1 peak was broader in this case. Interestingly however, on days 3 and 10, the distribution varied quite a lot from that of the

Fig.12a. The distribution of cells throughout the cell cycle in the healthy individual on day 3. The first panel shows the shape of the cells (granularity vs size). The second panel shows the distribution of the cells in G1- (E), S- (F), and G2/M- (G) phase of the cycle. The number of cells counted and the percentage of the cells in each phase is shown in the table below the panels.

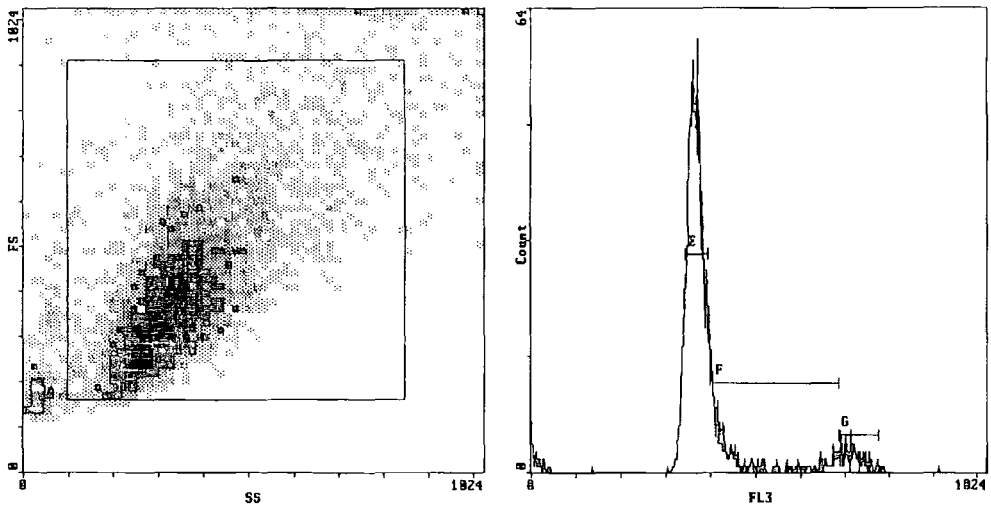

Stats: Normalized, Listgating: Disabled

Hist	Region	ID	%	Count	Mn X	Mn Y	PkPosX	PkPosY	PkCnt	FPCVX	FPCVY
1	A	A	86.6	3331	350.5	402.5	304.0	304.0	27	36.33	40.18

Hist	Region	ID	%	Count	Mn X	Md X	PkPosX	PkCnt	HPCV	Min	Max
4	E	E	61.6	2052	365.9	365.4	371.0	62	3.53	342.0	392.0
	F	F	15.9	531	497.5	450.2	416.0	15	0.18	404.0	686.0
	G	G	6.33	211	722.2	719.4	690.0	8	0.10	686.0	776.0

Fig.12b. The distribution of cells throughout the cell cycle in the healthy individual on day 5. The first panel shows the shape of the cells (granularity vs size). The second panel shows the distribution of the cells in G1- (E), S- (F), and G2/M- (G) phase of the cycle. The number of cells counted and the percentage of the cells in each phase is shown in the table below the panels.

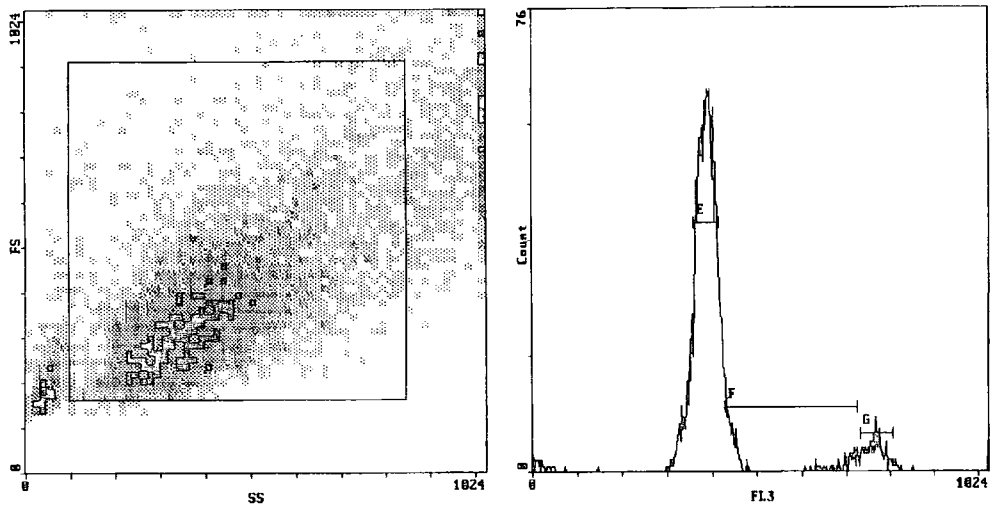

Stats: Normalized, Listgating: Disabled

Hist	Region	ID	%	Count	Mn X	Mn Y	PkPosX	PkPosY	PkCnt	FPCVX	FPCVY
1	A	A	78.1	4488	412.9	374.1	304.0	320.0	24	37.78	37.45

Hist	Region	ID	%	Count	Mn X	Md X	PkPosX	PkCnt	HPCV	Min	Max
4	E	E	63.2	2837	386.8	387.1	390.0	76	3.78	358.0	414.0
	F	F	9.27	416	524.9	450.5	428.0	21	8.18	428.0	726.0
	G	G	6.31	283	766.2	767.2	769.0	11	0.16	732.0	806.0

Fig.12c. The distribution of cells throughout the cell cycle in the healthy individual on day 10. The first panel shows the shape of the cells (granularity vs size). The second panel shows the distribution of the cells in G1- (E), S- (F), and G2/M- (G) phase of the cycle. The number of cells counted and the percentage of the cells in each phase is shown in the table below the panels.

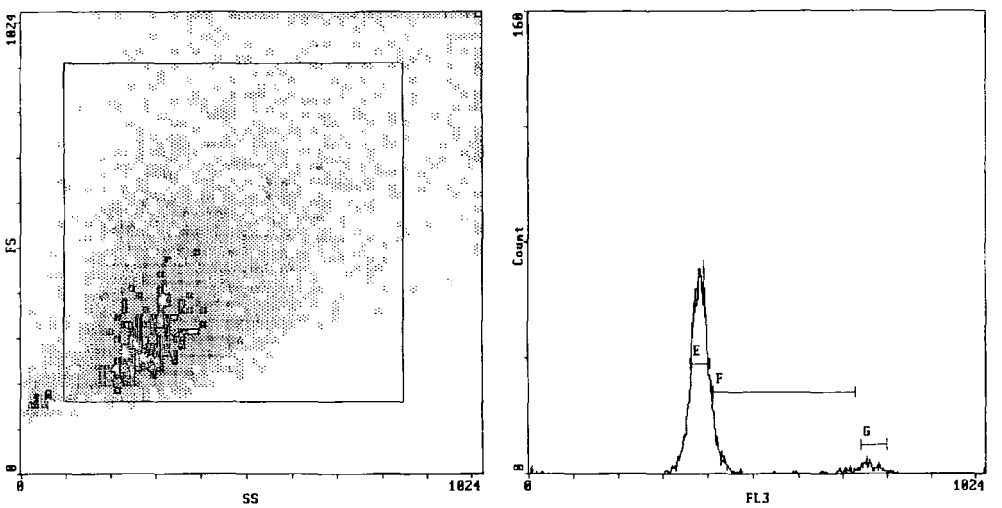

Stats: Normalized, Listgating: Disabled

Hist	Region	ID	%	Count	Mn X	Mn Y	PkPosX	PkPosY	PkCnt	FPCVX	FPCVY
1	A	A	88.3	3742	342.6	382.8	304.0	256.0	24	39.19	39.58

Hist	Region	ID	%	Count	Mn X	Md X	PkPosX	PkCnt	HPCV	Min	Max
4	E	E	66.5	2487	382.0	382.1	380.0	80	4.11	360.0	404.0
	F	F	12.0	449	472.6	424.3	410.0	28	6.55	410.0	728.0
	G	G	4.46	167	764.3	761.2	755.0	9	0.08	740.0	800.0

Fig.13a. The distribution of cells throughout the cell cycle in X-EDMD1 on day 3. The first panel shows the shape of the cells (granularity vs size). The second panel shows the distribution of the cells in G1- (E), S- (F), and G2/M- (G) phase of the cycle. The number of cells counted and the percentage of the cells in each phase is shown in the table below the panels.

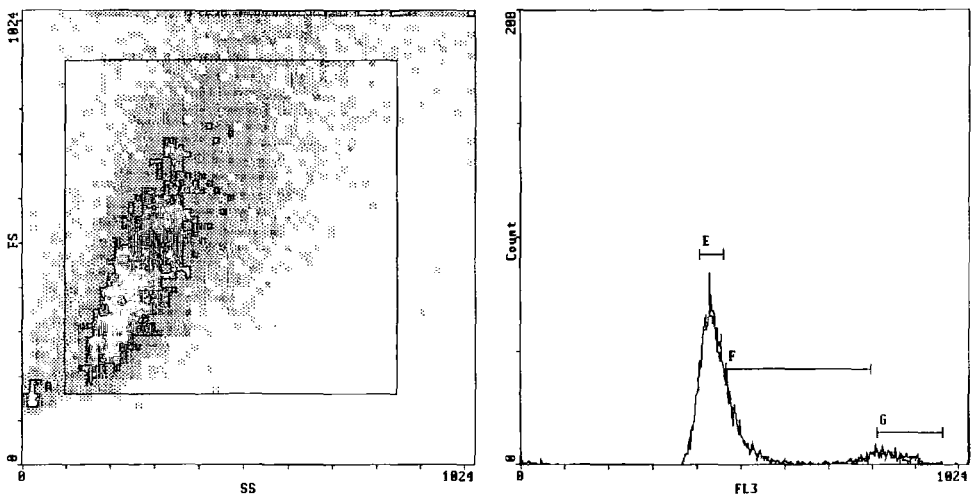

Stats: Normalized, Listgating: Disabled

Hist	Region	ID	%	Count	Mn X	Mn Y	PkPosX	PkPosY	PkCnt	FPCVX	FPCVY
1	A	A	85.1	6568	300.9	481.4	224.0	288.0	37	37.61	35.61

Hist	Region	ID	%	Count	Mn X	Md X	PkPosX	PkCnt	HPCV	Min	Max
4	E	E	50.6	3325	430.9	430.6	428.0	104	2.33	404.0	458.0
	F	F	26.4	1734	534.9	494.7	464.0	47	6.88	464.0	796.0
	G	G	7.19	472	860.8	852.9	823.0	10	0.11	810.0	962.0

Fig.13b. The distribution of cells throughout the cell cycle in X-EDMD1 on day 5. The first panel shows the shape of the cells (granularity vs size). The second panel shows the distribution of the cells in G1- (E), S- (F), and G2/M- (G) phase of the cycle. The number of cells counted and the percentage of the cells in each phase is shown in the table below the panels.

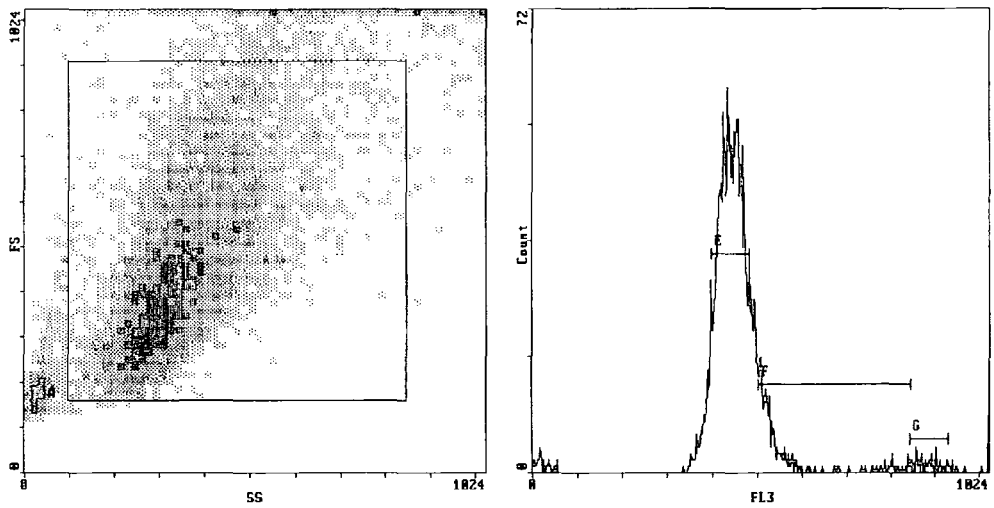

Stats: Normalized, Listgating: Disabled

Hist	Region	ID	%	Count	Mn X	Mn Y	PkPosX	PkPosY	PkCnt	FPCVX	FPCVY
1	A	A	83.9	5405	354.9	466.3	304.0	336.0	32	32.71	36.77

Hist	Region	ID	%	Count	Mn X	Md X	PkPosX	PkCnt	HPCV	Min	Max
4	E	E	67.0	3620	441.3	441.6	435.0	72	5.41	398.0	482.0
	F	F	12.9	698	571.7	528.6	509.0	21	10.39	502.0	844.0
	G	G	2.37	128	882.9	881.5	856.0	5	0.19	842.0	930.0

Fig.13c. The distribution of cells throughout the cell cycle in X-EDMD1 on day 10. The first panel shows the shape of the cells (granularity vs size). The second panel shows the distribution of the cells in G1- (E), S- (F), and G2/M- (G) phase of the cycle. The number of cells counted and the percentage of the cells in each phase is shown in the table below the panels.

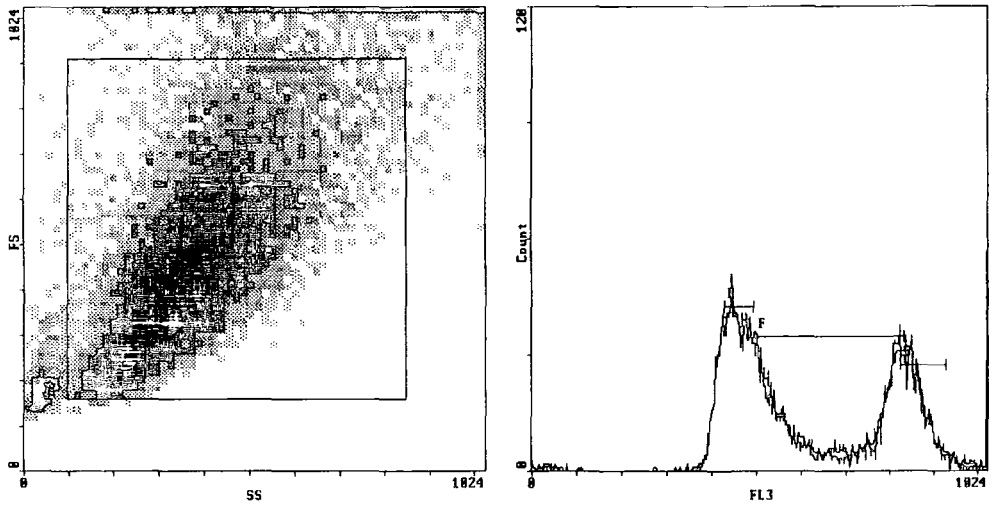

Stats: Normalized, Listgating: Disabled

Hist	Region	ID	%	Count	Mn X	Mn Y	PkPosX	PkPosY	PkCnt	FPCVX	FPCVY
1	A	A	87.7	9920	369.6	458.1	320.0	352.0	46	34.99	36.56

Hist	Region	ID	%	Count	Mn X	Md X	PkPosX	PkCnt	HPCV	Min	Max
4	E	E	26.2	2600	460.2	459.2	445.0	59	4.18	428.0	494.0
	F	F	41.9	4159	666.0	658.8	501.0	41	9.34	498.0	832.0
	G	G	19.3	1912	860.5	855.7	847.0	39	0.97	824.0	928.0

control with less cells found at G1 and more at S-phase compared to the control. Moreover, on day 10, a peak was observed at S-G2 phase of the cycle, which was quite similar to the G0-G1 one. Finally, on day 10 there were more cells at G2 phase than on day 3 and 5 and compared to the control as well. The granularity and the size of fibroblasts remained the same on all three days. The percentage of cells in each phase of the cycle for each day of analysis is shown in Figure 13. On day 3 (Fig. 13a) 50.6% of the cells were in G1, 26.4% were in S, and 7.19% were in G2/M (85.1% cells counted). On day 5 (Fig. 13b), 67% of the cells were in G1, 12.9% were in S, and 2.37% were in G2/M (83.9% cell counted). Finally, on day 10 (Fig. 13c), 26.2% of the cells were in G1, 41.9% were in S, and 19.3% were in G2/M (87.7% cells counted). The distribution of cells at passage 8 was as at passage 7. At passage 9, the cells appeared to be larger and more granular than at passage 7. Except from the broader than normally G0-G1 peak observed again at passage 9, the cell cycle distribution here was similar to that at passage 7 on day 3. On day 5 however, a second peak was again observed in S-G2 phase which persisted on day 10 as well. Data from passage 8 and passage 9 is not shown here.

The distribution of fibroblasts throughout the cell cycle in X-EDMD Carrier seemed to be quite similar to that of X-EDMD1 patient on day 3 at passages 7, 8 and 9 with the broad G0-G1 peak appearing here again. More specifically, on day 3 cells seemed to progress slower through S-phase compared to the control. On day 5 however and even more on day 10, the percentage of cells in S-phase decreased while that of G1-phase increased, resembling the control. The morphology of the cells was the same as in X-EDMD1 patient. Data collected from this patient at passage 7 is shown in Figure 14. On day 3 (Fig. 14a) 42.9% of the cells were in G1, 30.7% were in S, and 7.39% were in G2/M (88.9% cells counted). On day 5 (Fig. 14b), 64.2% of the cells were in G1, 19.5% were in

Fig.14a. The distribution of cells throughout the cell cycle in X-EDMD Carrier on day 3. The first panel shows the shape of the cells (granularity vs size). The second panel shows the distribution of the cells in G1- (E), S- (F), and G2/M- (G) phase of the cycle. The number of cells counted and the percentage of the cells in each phase is shown in the table below the panels.

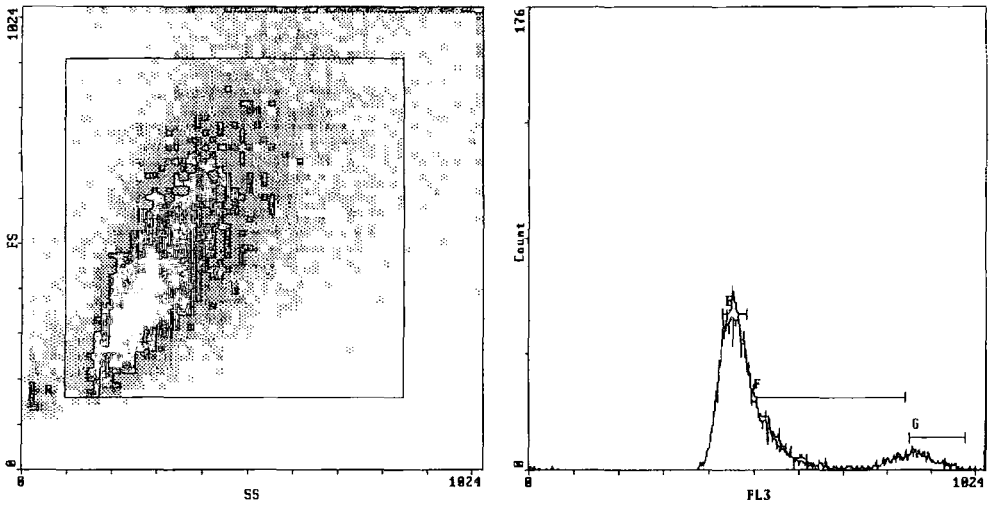

Stats: Normalized, Listgating: Disabled

Hist	Region	ID	%	Count	Mn X	Mn Y	PkPosX	PkPosY	PkCnt	FPCVX	FPCVY
1	A	A	88.9	7115	338.4	471.7	272.0	384.0	44	38.04	36.18

Hist	Region	ID	%	Count	Mn X	Md X	PkPosX	PkCnt	HPCV	Min	Max
4	E	E	42.9	3050	454.4	454.4	450.0	85	0.92	428.0	482.0
	F	F	30.7	2186	587.4	542.5	493.0	41	7.63	492.0	840.0
	G	G	7.39	526	895.4	888.2	866.0	13	0.26	850.0	976.0

Fig.14b. The distribution of cells throughout the cell cycle in X-EDMD Carrier on day 5. The first panel shows the shape of the cells (granularity vs size). The second panel shows the distribution of the cells in G1- (E), S- (F), and G2/M- (G) phase of the cycle. The number of cells counted and the percentage of the cells in each phase is shown in the table below the panels.

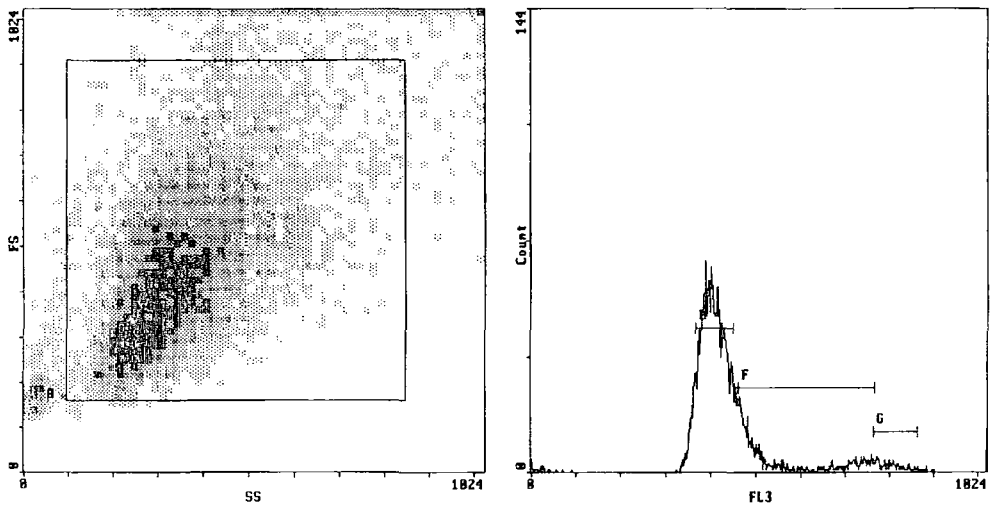

Stats: Normalized, Listgating: Disabled

Hist	Region ID	%	Count	Mn X	Mn Y	PkPosX	PkPosY	PkCnt	FPCVX	FPCVY
1	A A	88.5	5989	348.8	450.0	256.0	320.0	31	36.18	36.08

Hist	Region ID	%	Count	Mn X	Md X	PkPosX	PkCnt	HPCV	Min	Max
4	E E	64.2	3842	406.5	404.9	388.0	70	6.45	366.0	450.0
	F F	19.5	1165	561.9	507.1	466.0	28	10.20	462.0	766.0
	G G	3.76	225	803.6	801.7	776.0	7	0.08	764.0	862.0

Fig.14c. The distribution of cells throughout the cell cycle in X-EDMD Carrier on day 10. The first panel shows the shape of the cells (granularity vs size). The second panel shows the distribution of the cells in G1- (E), S- (F), and G2/M- (G) phase of the cycle. The number of cells counted and the percentage of the cells in each phase is shown in the table below the panels.

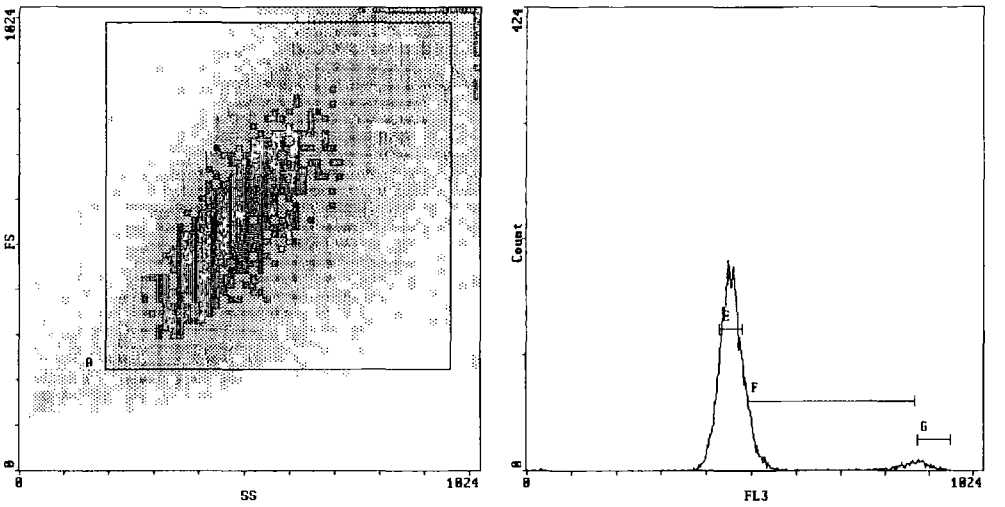

Stats: Normalized, Listgating: Disabled

Hist	Region	ID	%	Count	Mn X	Mn Y	PkPosX	PkPosY	PkCnt	FPCVX	FPCVY
1	A	A	85.8	12343	535.1	572.9	448.0	608.0	31	28.85	30.75

Hist	Region	ID	%	Count	Mn X	Md X	PkPosX	PkCnt	HPCV	Min	Max
4	E	E	63.1	7787	453.8	453.6	449.0	210	4.50	428.0	480.0
	F	F	14.3	1762	593.3	513.8	492.0	65	7.81	492.0	868.0
	G	G	2.65	327	897.1	892.6	876.0	16	0.08	874.0	948.0

S, and 3.76% were in G2/M (88.5% cells counted). Finally, on day 10 (Fig. 14c), 63.1% of the cells were in G1, 14.3% were in S, and 2.65% were in G2/M (85.8% cells counted).

In X-EDMD2 patient (Fig.15) the pattern of distribution was normal at all passages with the G0-G1 peak being sharper here and the whole pattern being very similar to that of the control fibroblasts. Data shown in Figure 15 is from passage 7. On day 3 (Fig. 15a) 57.3% of the cells were in G1, 16.3% were in S, and 3.08% were in G2/M (93.7% cells counted). On day 5 (Fig. 15b), 53.5% of the cells were in G1, 10.8% were in S, and 2.31% were in G2/M (75.5% cells counted). Finally, on day 10 (Fig. 15c), 59.5% of the cells were in G1, 18.1% were in S, and 2.4% were in G2/M (84.4% cells counted).

Data collected from AD-EDMD patient from passages 7, 8 and 9 showed that the distribution of these cells was different from that of the control with the broad peak in Go-G1 phase being present here again. Fibroblasts of this patient seemed to progress slower through S-phase as in X-EDMD1 and X-EDMD Carrier. Furthermore, accumulation at confluence was observed at G1-phase as in the X-EDMD Carrier. Representative data from this patient at passage 7 is shown in Figure 16. On day 3 (Fig. 16a) 55.5% of the cells were in G1, 21.9% were in S, and 4.03% were in G2/M (90% cells counted). On day 5 (Fig. 16b), 47.6% of the cells were in G1, 21.6% were in S, and 4.81% were in G2/M (95.3% cells counted). Finally, on day 10 (Fig. 16c), 63.1% of the cells were in G1, 25.4% were in S, and 5.66% were in G2/M (92.4% cells counted). Cell morphology was the same as in the other patients.

Fig.15a. The distribution of cells throughout the cell cycle in X-EDMD2 on day 3. The first panel shows the shape of the cells (granularity vs size). The second panel shows the distribution of the cells in G1- (E), S- (F), and G2/M - (G) phase of the cycle. The number of cells counted and the percentage of the cells in each phase is shown in the table below the panels.

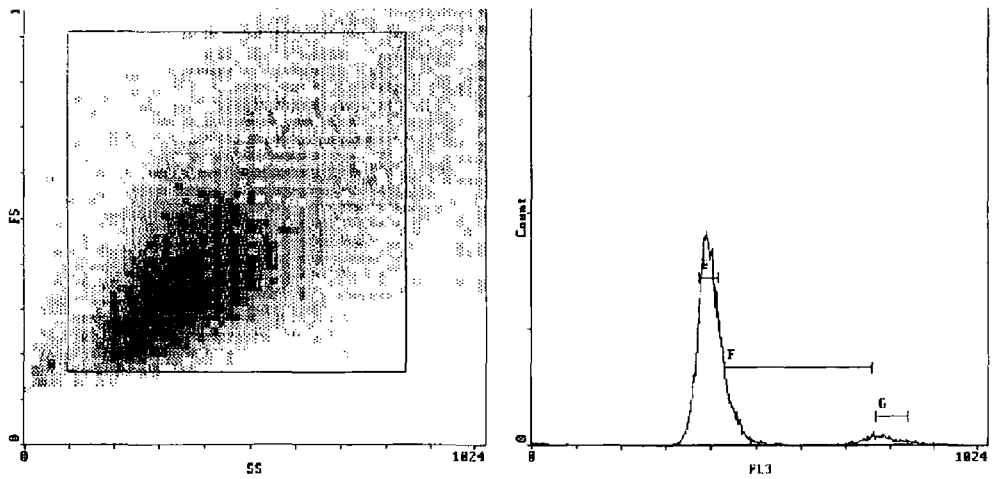

Normalized, Listgating: Disabled

Region	ID	%	Count	Mn X	Mn Y	PkPosX	PkPosY	PkCnt	FPCVX	FPCVY
A	A	93.7	15176	381.0	378.9	288.0	288.0	84	35.23	36.25

Region	ID	%	Count	Mn X	Md X	PkPosX	PkCnt	HPCV	Min	Max
E	E	57.3	8700	393.8	393.5	390.0	250	5.18	372.0	416.0
F	F	16.3	2468	492.1	450.6	431.0	93	8.36	430.0	760.0
G	G	3.08	468	798.7	795.3	779.0	14	0.75	770.0	840.0

Fig.15b. The distribution of cells throughout the cell cycle in X-EDMD2 on day 5. The first panel shows the shape of the cells (granularity vs size). The second panel shows the distribution of the cells in G1- (E), S- (F), and G2/M- (G) phase of the cycle. The number of cells counted and the percentage of the cells in each phase is shown in the table below the panels.

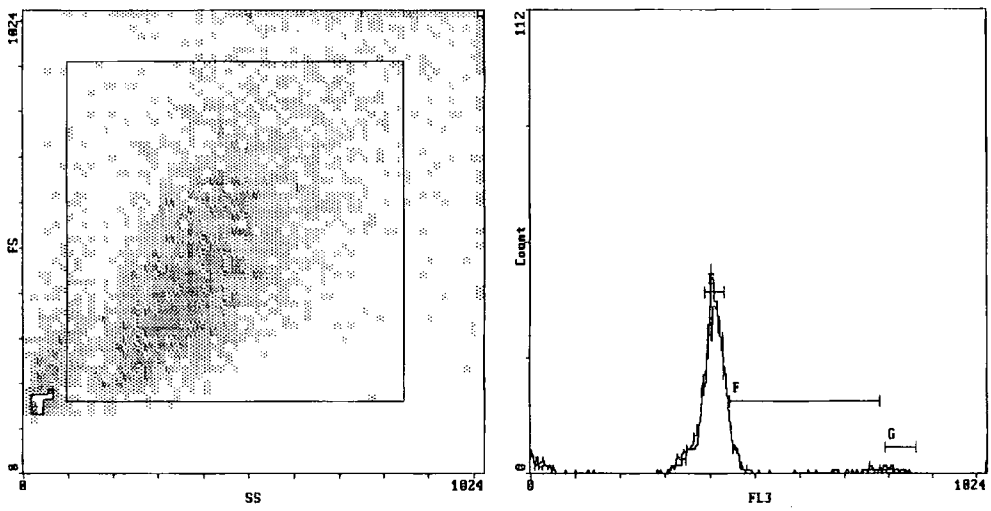

Stats: Normalized, Listgating: Disabled

Hist	Region	ID	%	Count	Mn X	Mn Y	PkPosX	PkPosY	PkCnt	HPCVX	HPCVY
1	A	A	75.5	2947	391.8	466.5	304.0	288.0	14	35.96	36.16

Hist	Region	ID	%	Count	Mn X	Md X	PkPosX	PkCnt	HPCV	Min	Max
4	E	E	53.5	1576	410.0	409.8	402.0	54	2.82	388.0	432.0
	F	F	10.8	318	543.8	463.0	448.0	18	0.15	444.0	780.0
	G	G	2.31	68	814.8	811.2	797.0	4	0.09	792.0	862.0

Fig.15c. The distribution of cells throughout the cell cycle in X-EDMD2 on day 10. The first panel shows the shape of the cells (granularity vs size). The second panel shows the distribution of the cells in G1- (E), S- (F), and G2/M- (G) phase of the cycle. The number of cells counted and the percentage of the cells in each phase is shown in the table below the panels.

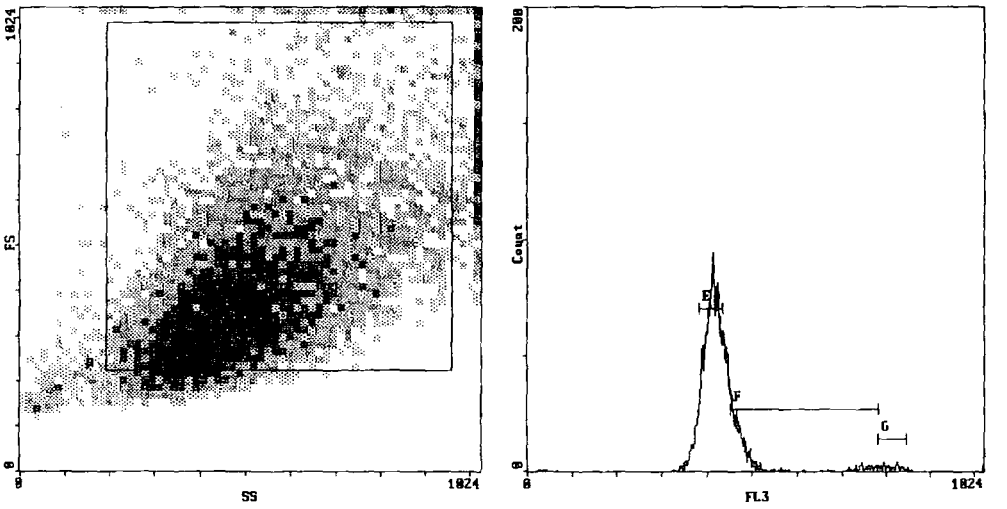

Stats: Normalized, Listgating: Disabled

Hist	Region	ID	%	Count	Mn X	Mn Y	PkPosX	PkPosY	PkCnt	FPCVX	FPCVY
1	A	A	84.4	5926	518.7	417.0	352.0	224.0	23	30.13	36.08

Hist	Region	ID	%	Count	Mn X	Md X	PkPosX	PkCnt	HPCV	Min	Max
4	E	E	59.5	3526	411.2	412.0	414.0	97	5.00	382.0	436.0
	F	F	18.1	1074	511.8	473.6	454.0	39	7.69	452.0	782.0
	G	G	2.40	142	811.4	809.5	807.0	6	0.06	782.0	846.0

Fig.16a. The distribution of cells throughout the cell cycle in AD-EDMD on day 3. The first panel shows the shape of the cells (granularity vs size). The second panel shows the distribution of the cells in G1- (E), S- (F), and G2/M- (G) phase of the cycle. The number of cells counted and the percentage of the cells in each phase is shown in the table below the panels.

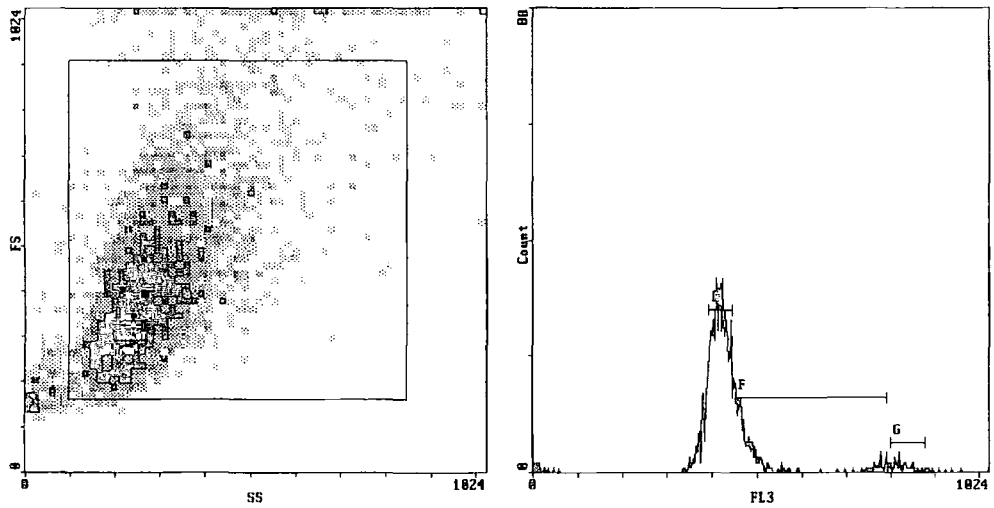

Stats: Normalized, Listgating: Disabled

Hist	Region	ID	%	Count	Mu X	Mn Y	PkPosX	PkPosY	PkCnt	FPCVX	FPCVY
1	A	A	90.0	2704	286.4	425.1	224.0	320.0	20	37.57	37.79

Hist	Region	ID	%	Count	Mn X	Md X	PkPosX	PkCnt	HPCV	Min	Max
4	E	E	55.5	1501	417.9	417.7	408.0	43	2.03	392.0	444.0
	F	F	21.9	593	523.6	477.8	454.0	21	0.73	452.0	790.0
	G	G	4.03	109	830.3	828.0	819.0	6	0.08	798.0	878.0

Fig.16b. The distribution of cells throughout the cell cycle in AD-EDMD on day 5. The first panel shows the shape of the cells (granularity vs size). The second panel shows the distribution of the cells in G1- (E), S- (F), and G2/M- (G) phase of the cycle. The number of cells counted and the percentage of the cells in each phase is shown in the table below the panels.

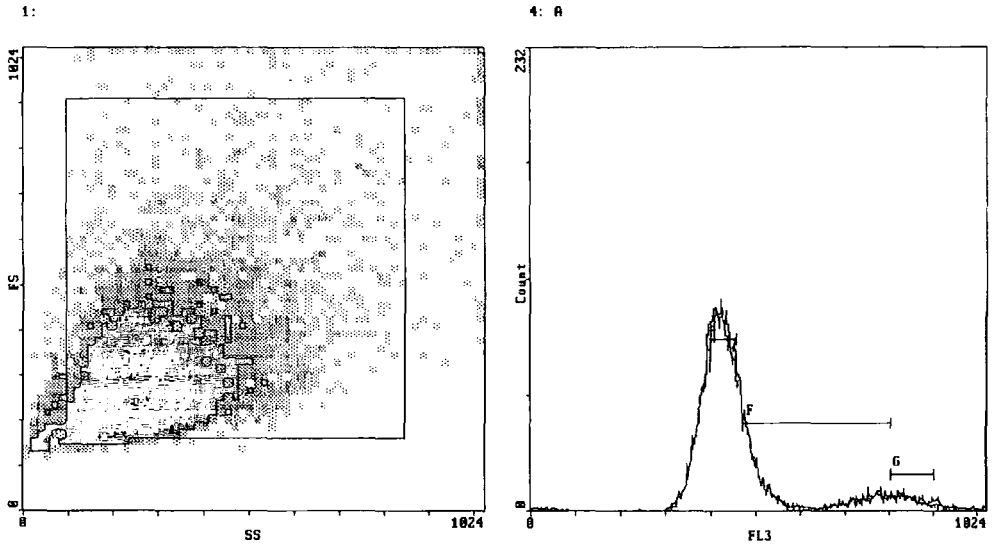

Stats: Normalized, Listgating: Disabled

Hist	Region	ID	%	Count	Mn X	Mn Y	PkPosX	PkPosY	PkCnt	FPCVX	FPCVY
1	A	A	95.3	12932	265.5	269.1	224.0	192.0	162	39.44	39.86

Hist	Region	ID	%	Count	Mn X	Md X	PkPosX	PkCnt	HPCV	Min	Max
4	E	E	47.6	6158	423.4	423.0	395.0	113	8.51	390.0	458.0
	F	F	21.6	2792	578.6	518.0	475.0	53	11.98	472.0	802.0
	G	G	4.81	622	846.2	843.2	804.0	14	0.09	802.0	902.0

Fig.16c. The distribution of cells throughout the cell cycle in AD-EDMD on day 10. The first panel shows the shape of the cells (granularity vs size). The second panel shows the distribution of the cells in G1- (E), S- (F), and G2/M- (G) phase of the cycle. The number of cells counted and the percentage of the cells in each phase is shown in the table below the panels.

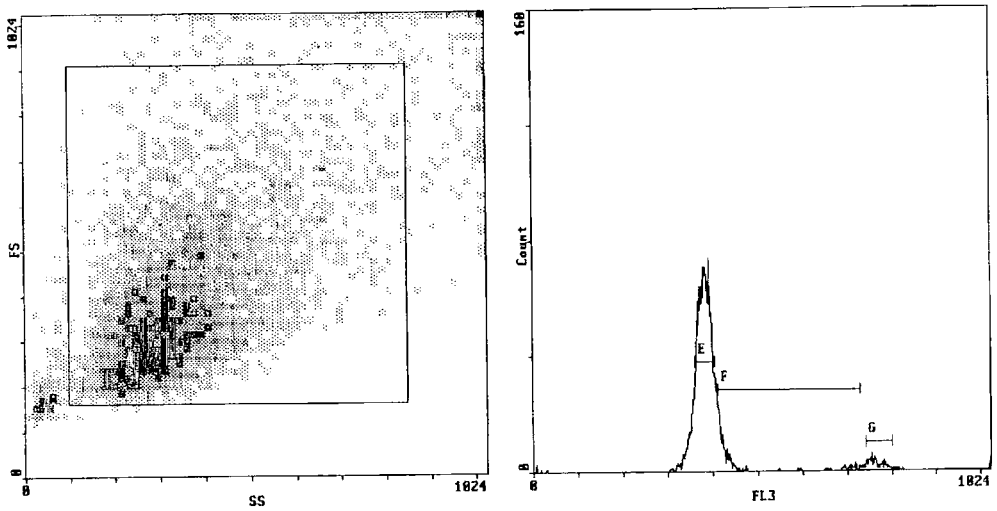

Stats: Normalized, Listgating: Disabled

Hist	Region	ID	%	Count	Mn X	Mn Y	PkPosX	PkPosY	PkCnt	FPCVX	FPCVY
1	A	A	88.3	3742	342.6	382.8	304.0	256.0	24	39.19	39.58

Hist	Region	ID	%	Count	Mn X	Md X	PkPosX	PkCnt	HPCV	Min	Max
4	E	E	66.5	2487	382.0	382.1	380.0	80	4.11	360.0	404.0
	F	F	12.0	449	472.6	424.3	410.0	28	6.55	410.0	728.0
	G	G	4.46	167	764.3	761.2	755.0	9	0.08	740.0	800.0

Discussion

Immunocytochemistry of LCLs

The normal cellular distribution of lamins and emerin has been shown to be affected in muscle cells taken from patients with EDMD. From the immunofluorescence microscopy results of lymphoblasts taken from EDMD patients and healthy individuals, (Table 6, 7, 8, and 9), it is possible that the same holds for lymphoblastoid cells as well. However, only one control LCL was available for the experiments conducted, Burkitts lymphoma being an established cell line with clear differences in lamin A expression. This, and the variability of the EDMD LCLs makes it difficult to evaluate the significance of the differences for EDMD, without a large number of control LCLs.

More specifically, in the two AD-EDMD patients' LCLs, the mutation on the lamin A/C gene is found on exon 9, and affects the expression of lamin A protein, whereas lamin C production does not appear to be affected by the mutation. Lamin A as seen from Table 6, was translocated to the cytoplasm in both patients, in a significant number of cells scored. From experiments conducted previously, it has been shown that the distribution of lamin B1 and B2 is not affected by absence/deficiency of lamin A, implying that A- and B-type lamins' possible interactions are not essential for the assembly and maintenance of the nuclear lamina. From this finding it can also be assumed that lamin A is not involved directly in the localization of B-type lamins. Comparing the results of the two AD-EDMD cell lines however with that of control LCL cell line, it can be seen that in these experiments B-type lamins were affected by the translocation of lamin A. A higher number of cells showing cytoplasmic staining for B-type lamins was seen in the two AD-EDMD cell lines examined compared to control LCL cell line. The distribution of lamin C was clearly seen to be only slightly affected by the mutation of lamin A as shown in Table 5 and

when compared to Burkitts lymphoma and control LCL cell lines. However, as seen in Table 9, in the case of Burkitts lymphoma cell line lamin C was absent (no staining occurred) or was found in very few cells, giving a very dull staining of nuclei. The above indicate a possible interaction between lamin A and lamin C, which may be involved in the localization of lamin C. Although absence of lamin C was unexpected, it has been previously speculated (Hutchison et al., 2001) that lamin A stabilizes lamin C. Mutations in lamin A/C gene therefore resulting in absence/deficiency of lamin A, could lead to the dissociation of lamin C with the nucleus and consequently translocation of lamin C from the NE to the cytoplasm. Furthermore, absence of lamin C from cells could be the result of degradation following disassociation of the protein with the nucleus. It should be noted at this point that the results collected for the two AD-EDMD patients do not strongly support the above speculations since in those cases there is no great change in lamin C distribution. However, it can be assumed that the mutations in these two patients are not located in sites critical for the lamin A-lamin C interaction.

Recently, it has been shown that lamin A binds directly to emerin in vitro (Clements et al., 2000). Taking this into account, the results summarized in Table 6 were as expected. Emerin in both EDMD cell lines was localized in the cytoplasm in a diffused form in a high proportion of cells compared to control LCL, and being very similar to Burkitts lymphoma, while dull staining on the nuclear envelope has also been observed. This is possibly due to emerin not been anchored to the nuclear envelope because of the mutation in lamin A/C gene. Redistribution of emerin was expected because previous studies indicate that lamin A/C anchors emerin at the NE (Sullivan et al., 1999). Finally, emerin has also been shown to interact with B-type lamins. Diffusion of lamins in the cytoplasm in a proportion of cells seen in both AD-EDMD cell lines as well as Burkitts lymphoma, could therefore be explained as misanchoring of B-type lamin to the NE.

From Table 7 in which the results of the X-linked EDMD patients are summarized, emerin staining was only seen in patient X-1. Mutations in all other patients resulted in no emerin expression at all and thus no staining occurred. In these patients, lamin C was seen to be slightly affected. This indicates that there is possible interaction between emerin and lamin C and is thus in agreement with the prediction made by Vaughan and coworkers (Vaughan et al., 2001). In all patients' cell lines, some or all lamins (lamin A, B1, and B2) were seen to be affected. Although loss of lamin A and B-type lamins to the cytoplasm was unexpected, it may again suggest that in these cells emerin influence lamins association with the nucleus. However, no general pattern can be seen and thus no firm conclusion can be drawn.

From the data collected from sporadic EDMD patients (Table 8), no general pattern of distribution of the lamins could again be identified and therefore no conclusion can be drawn from these results either. However, it is interesting to note that in this case in four out of the ten patients examined in total, emerin was not localized in the nuclear envelope nor was it diffused in the cytoplasm. In S-1 and S-2 patients, the majority of the cells were not stained with the emerin antibody, whereas in S-6 and S-10 patients, emerin appeared to be diffused inside the nucleus. This result suggests two possible explanations; Degradation of emerin due to instability of assembly with the NE, and/or deficient transport of the protein through the endoplasmic reticulum. The results obtained here are very interesting and require further investigation of the four cell lines.

Immunocytochemistry of fibroblasts

In order to investigate the distribution of emerin, lamin A and lamin C in fibroblasts of EDMD patients, four cell lines of patients' fibroblasts and one of a healthy individual were transfected with GFP-emerin, GFP-LA and DsRed-LC constructs. As was clearly

shown in these experiments and can be seen from Figure 8, 9 10, and 11, the distribution of transfected lamin A, lamin C and emerin, does not appear to be affected in the cell lines examined. Data collected from the normal fibroblasts, is the same as that collected from the EDMD cell lines. In all five cell lines the GFP-emerin construct was seen both in the nuclear rim and diffused in the cytoplasm. GFP-LA, and DsRed-LC on the other hand were both found in the nuclear rim while DsRed-LC was also seen in patches inside the nucleus. Overall, using this approach no abnormalities in lamin assembly pathways were observed (Ostlund et al., 2001). Apart from all the above however, when interpreting the results, it should be taken into account that the transfection efficiency was very low. Only 5% of the total population of cells was transfected. More experiments therefore on the same cell lines have to be conducted optimizing the conditions of electroporation so that higher transformation efficiencies are reached.

While some evidence of structural abnormality was observed in LCLs, none was seen in fibroblasts. Perhaps the effect if any on LCLs and even more on fibroblasts, is weak and would only be observed in muscle cells. Therefore ideally the experiments should be repeated in skeletal muscle. The current data does not lend strong support to the hypothesis that EDMD arises from weakness of the lamina (Hutchison et al., 2001).

Overall, from the immunocytochemistry experiments on lymphoblasts conducted, one can conclude that although some differences are suggested in EDMD, much more study is required before the possibility of using such differences for diagnosis can be considered. Furthermore, transfection of fibroblasts did not show up any differences between EDMD and control cells that might be useful in diagnosis. Finally, more experiments have to be designed and performed in order to investigate the causes of muscular dystrophy in

sporadic EDMD patients, and to explain the absence/deficiency of emerin observed in the lymphoblasts of the four out of the ten patients examined in this study.

The nuclear lamina and cell cycle effects in EDMD cells

Nuclear lamins have been speculated to be involved in the progression of the cell through the cell cycle by playing a central role in the assembly of the nuclear envelope and growth. Emerin has also been found to exist in the cell in four phosphorylated forms, out of which three have been shown to be associated with the cell cycle. According thus to the above and if these assumptions are true, it would be expected that mutations in the genes encoding lamins and emerin would have an effect of some kind on the progression of the cells through the different phases of the cycle. FACS analysis was thus performed on fibroblastic cell lines taken from patients with AD- and X-linked EDMD to investigate whether or not there is an effect on the cell cycle.

From the results section and figures 12-16, it can be clearly seen that there is a significant difference in the distribution of cells around the cycle amongst the five different cell lines. The four patients' cell lines had one feature in common in their distribution which was different from control cells. The peak at the G0-G1 phase of the cycle was much broader in these cell lines compared to the control, and although it was less broad in the case of X-EDMD2 patient, the difference was still evident. The same peak was very sharp for the control cell line. One feature that was very interesting and appeared in the distribution patterns of both X-EDMD1 and X-EDMD2 cell lines, was the peak that was seen at S-G2 phase of the cycle after 5 days in culture. These two patients had both mutations in the emerin gene. That peak was not however observed in X-EDMD Carrier and AD-EDMD cell lines, bearing mutations in emerin (carrier) and lamin A genes

respectively. The broader than normal peak seen in all EDMD cell lines could be explained in terms of cell cycle block or apoptosis. Cells may be accumulating at G0 phase of the cycle either because the mutation has been spotted and is lethal for the cells so they are going through apoptosis or because they are blocked by checking mechanisms. The second peak observed in S-G2 phase is clearly a cycle arrest. From the percentage of the cells in each phase of the cycle, it can be suggested that with the exception of X-EDMD2, emerin and lamin mutations cause cells to progress through S-phase slower than normal due to checking mechanisms/cycle arrest. That becomes more evident in the case of X-EDMD1 patient in which cells at confluence accumulate in S/G2- phase instead of G1 as in the control cells.

The above assumption of cell cycle arrest, can be explained in terms of the Rb protein. The most severe lamina abnormalities have been observed in X-EDMD patients. Moreover, lamins are shown to be Rb binding partners. Taking these two points into account, perhaps absence/mutation of lamin C or emerin, or both, causes mis-regulation of Rb and consequently cell cycle arrest.

At this point it should be noted that control and patient fibroblasts were compared by FACS with a manifesting carrier. The carrier will have a mixture of emerin expressing and emerin null cells, the majority being emerin expressing since manifesting. The carrier's cell cycle distribution of the cells should therefore be somewhere between the patient's and the control's but closer to the patient's one. Although this is a good internal control for the technique, it does not fit the expected pattern.

Although the differences between the five cell lines examined here may be genuine, the factor of variable penetrance has to be considered as well. In addition, when hypotheses about emerin effects on cell division are evaluated, the fact that people with no emerin at all (X-EDMD patients) grow to normal adult stature at normal rates must be considered.

Clearly, neither lack of emerin nor the pathogenic lamin A/C mutations have any significant effects on cell growth and cell number at the level of the whole organism.

In order to investigate further the effects of lamins and emerin mutations on the cells' cycle, more work needs to be conducted. Further immunocytochemical and biochemical experiments need to be performed and the work carried out here should be repeated using more cell lines from EDMD patients.

References

Belmont AS, Zhai Y, Thilenius A. (1993) Lamin B distribution and association with peripheral chromatin revealed by optical sectioning and electron microscopy tomography. J Cell Biol. 123:1671-85.

Betto R, Biral D, Sandona D. (1999) Functional roles of dystrophin and of associated proteins. New insights for the sarcoglycans. Ital J Neurol Sci. 20:371-9. Review.

Biamonti G, Giacca M, Perini G, Contreas G, Zentilin L, Weighardt F Guerra M, Della Valle G, Saccone S, Riva S, et al. (1992) The gene of a novel human lamin maps at a highly transcribed locus of chromosome 19 which replicates at the onset of S-phase. Mol Cell Biol. 12:3499-3506.

Bione S, Maestrini M, Rivella S, Mancini M, Regis S, Romeo G, Toniolo D (1994) Identification of a novel X-linked gene responsible for Emery Dreifuss muscular dystrophy. Nat Genet 8:323-327.

Bione S, Small K, Aksmanovic VMA, D'Urso M, Ciccodicola A, Merlini L, Morandi L, et al (1995) Identification of new mutations in the Emery Dreifuss muscular dustrophy gene and evidence of genetic heterogeneity of the disease. Hum Mol Genet. 4:1859-1863.

Bione S, D'Adamo P, Maestrini E, Gedeon AK, Bolhuis PA, Toniolo D (1996) A novel X-linked gene, G4.5. is responsible for Barth syndrome. Nat Genet. 12:385-9.

Bonne G, Raffaele di Barletta M, Varnous S, Becane HM, Hammouda EH, Merlini L, Muntoni F, et al (1999) Mutations in the gene encoding lamin A/C cause autosomal dominant Emery-Dreifuss muscular dystrophy. Nat Genet. 21:285-288.

Bridger JM, Kill IR, O'Farrel M, Hutchison CJ (1993) Internal lamin structures within G1 nuclei of dermal fibroblasts. J Cell Sci. 104:297-306.

Broers JL, Machiels BM, Kuijpers HJ, Smedts F, van den Kieboom R, Raymond Y, Ramaekers FC. (1997) A- and B-type lamins are differentially expressed in normal human tissues. Histochem Cell Biol. 107:505-17.

Cao H, Hegele RA. (2000) Nuclear lamin A/C R482Q mutation in canadian kindreds with Dunnigan-type familial partial lipodystrophy. Hum Mol Genet. 9:109-12.

Cartegni L, Raffaele di Barletta M, Barresi R, Squarzoni S, Sabatelli P, Maraldi N, Mora M, et al. (1997) Heart specific localisation of emerin: new insights into Emery-Dreifuss muscular dystrophy. Hum Mol Genet 6:2257-2264.

Clements L, Manilal S, Love DR, Morris GE. (2000) Direct interaction between Emerin and Lamin A. Biochem Biophys Res Com. 267:709-714.

Collas P, Courvalin JC, Poccia D. (1996) Targeting of membranes to sea urchin sperm chromatin is mediated by a lamin B receptor-like integral membrane protein. J Cell Biol. 135:1715-25.

Dabauvalle MC, Loos K, Merkert H, Scheer U. (1991) Spontaneous assembly of pore complex-containing membranes ("annulate lamellae") in Xenopus egg extract in the absence of chromatin. J Cell Biol. 112:1073-82.

Dabauvalle MC, Muller E, Ewald A, Kress W, Krohne G. (1999) Distribution of emerin during the cell cycle. Eur J Cell Biol. 78:749-756.

Dechat T, Korbei B, Vaughan AO, Vlcek S, Hutchison CJ, Foisner R. (2000) Intranuclear Lamina-associated Polypeptide 2α binds A-type lamins. J Cell Sci. 113(Pt19):3473-34784.

Ellenberg J, Siggia ED, Moreira JE, Smith CL, Presley JF, Worman HJ, Lippincott-Schwartz J. (1997) Nuclear membrane dynamics and reassembly in living cells: targeting of an inner nuclear membrane protein in interphase and mitosis. J Cell Biol. 138:1193-1206.

Ellis DJ, Jenkins H, Whitfield WG, Hutchison CJ. (1997) GST-fusion proteins act as dominant negative mutants in Xenopus egg extract and reveal the function of the lamina in DNA replication. L Cell Sci. 110:2507-2518.

Ellis JA, Craxton M, Yates JR, Kendrick-Jones J. (1998) Aberrant intracellular targeting and cell cycle-dependent phosphorylation of emerin contribute to the Emery-Dreifuss muscular dystrophy phenotype. J Cell Sci. 111:781-92.

Ellis JA, Craxton M, Yates JRW, Kendrick-Jones J, Brown C. (1999) GST-lamin fusion proteins act as dominant negative mutants in Xenopus egg extracts and reveal the function of the lamina in DNA replication. J Cell Sci. 110:2507-2518.

Emery AE. (1989) Emery-Dreifuss syndrome. J Med Genet 26:637-641.

Emery AE. (2000) Emery-Dreifuss muscular dystrophy - a 40 year retrospective. Neuromuscul Disord. 10:228-32. Review.

Fairley EAL, Kendrick-Jones J, Ellis JA. (1999) The Emery-Dreifuss muscular dystrophy phenotype arises from aberrant targeting and binding of emerin at the inner nuclear membrane. J Cell Sci. 122:2571-2582.

Farnsworth CC, Wolda SL, Gelb MH, Glomset JA. (1989) Human lamin B contains a farnesylated cysteine residue.J Biol Chem. 264:20422-9.

Fatkin D, MacRae C, Sasaki T, Wolff MR, Porcu M, Frenneaux M, Atherton J, Vidaillet HJ Jr, Spudich S, De Girolami U, Seidman JG, Seidman C, Muntoni F, Muehle G, Johnson W, McDonough B. (1999) Missense mutations in the rod domain of the lamin A/C gene as causes of dilated cardiomyopathy and conduction-system disease. N Engl J Med. 341:1715-24.

Fisher DZ, Chaudhary N, Blobel G. (1986) cDNA sequencing of nuclear lamins A and C reveals primary and secondary structural homology to intermediate filaments. Proc Natl Acad Sci USA. 83:6450-6454.

Foisner R, Gerace L (1993) Integral membrane proteins of the nuclear envelope interact with lamins and chromosomes, and binding is modulated by mitotic phosphorylation. Cell 73:1267-1279.

Foisner R. (1997) Dynamic organisation of intermediate filaments and associated proteins during the cell cycle. Bioessays. 19:297-305. Review.

Fricker M, Hollinshead M, White N, Vaux D. (1997) Interphase nuclei of many mammalian cell types contain deep, dynamic, tubular membrane bound invaginations of the nuclear envelope, J Cell Biol. 136:531-544.

Furukawa K, Hotta Y. (1993) cDNA cloning of a germ cell specific lamin B3 from mouse spermatocytes and analysis of its function by ectopic expression in somatic cells. EMBO J. 12:97-106.

Furukuwa K, Inagaka H, Hotta Y. (1994) Identification and cloning of an RNA coding for a germ cell-specific A-type lamin in mice. Exp Cell Res. 212:426-430.

Furukawa K, Pante N, Aebi U, Gerace L. (1995) Cloning of a cDNA for lamina-associated polypeptide 2 (LAP2) and identification of regions that specify targeting to the nuclear envelope. EMBO J. 14:1626-36.

Gant TM, Wilson KL (1997) Nuclear assembly. Annu Rev Cell Dev Biol. 13:669-695.

Georgatos SD, Pyrpasopoulou A, Theodoropoulos PA. (1997) Nuclear envelope breakdown in mammalian cells involves stepwise lamina disassembly and microtubule-drive deformation of the nuclear membrane.J Cell Sci. 110:2129-40.

Gerace L, Blobel G. (1980) The nuclear envelope lamina is reversibly depolymerized during mitosis. Cell. 19:277-87.

Gerace L, Burke B. (1988) Functional organisation of the nuclear envelope. Annu Rev Cell Biol. 4:335-374.

Gerace L, Foisner R. (1994) Integral membrane proteins and dynamic organisation of the nuclear envelope. Trends Cell Biol. 4:127-131.

Glass CA, Glass JR, Taniura H, Hasel KW, Blevitt JM, Gerace L. (1993) The alpha-helical rod domain of human lamins A and C contains a chromatin binding site. EMBO J. 12:4413-24.

Goldberg M, Harel A, Gruenbaum Y. (1999) The nuclear lamina: molecular organization and interaction with chromatin. Crit Rev Eukaryot Gene Expr. 9:285-93. Review.

Hacia JG, Collins FS. (1999) Mutational analysis using oligonucleotide microarrays. J Med Genet. 36:730-6. Review.

Harel A, Goldberg M, Ulitzur N, Gruenbaum Y. (1998) Structural organization and biological roles of the nuclear lamina. In: Textbook of Gene Therapy and Molecular

Biolog: From Basic Mechanism to Clinical Applications, ed. T. Boulikas, Palo Ito, CA: Gene Therapy Press. 1:529-542.

Harris CA, Andryuk PJ, Cline SW, Mathew S, Siekerka JJ, Goldstein G. (1995) Structure and mapping of the human thymopoietin (TMPO) gene and relationship of human TMPO beta to rat lamin-associated polypeptide 2. Genomics. 20:198-205.

Heins S, Aebi U. (1994) Making heads and tails of intermediate filament assembly, dynamics and networks. Curr Opin Cell Biol. 6:25-33. Review.

Hennekes H, Peter M, Weber K, Nigg EA. (1993) Phosphorylation on protein kinase C sites inhibits nuclear import of lamin B2.J Cell Biol. 120:1293-304.

Hess JF, Casselman JT, Kong AP, FitzGerald PG. (1998) Primary sequence, secondary structure, gene structure, and assembly properties suggests that the lens-specific cytoskeletal protein filensin represents a novel class of intermediate filament protein. Exp Eye Res. 66:625-44.

Hoger TH, Krohne G, Kleinschmidt JA. (1991) Interaction of Xenopus lamins A and LII with chromatin in vitro mediated by a sequence element in the carboxyterminal domain. Exp Cell Res. 197:280-9.

Holt I, Clements L, Manilal S, Brown SC, Morris GE. (2001) The R482Q lamin A/C mutation that causes lipodystrophy does not prevent nuclear targeting of lamin A in adipocytes or its interaction with emerin. Eur J Hum Genet. 9:204-8.

Hutchison CJ, Bridger JM, Cox LS, Kill IR. (1994) Weaving a pattern from disparate threads: lamin function in nuclear assembly and DNA replication. J Cell Sci. 107:3259-69. Review.

Hutchison CJ, Alvarez-Reyes M, Vaughan OA. (2001) Lamins in disease: why do ubiquitously expressed nuclear envelope proteins give rise to tissue-specific disease phenotypes? J Cell Sci. 114:9-19. Review.

Izumi M, Vaughan OA, Hutchison CJ, Gilbert DM. (2000) Head and/or CaaX domain deletions of lamin proteins disrupt preformed lamin A and C but not lamin B structure in mammalian cells. Mol Biol Cell. 11:4323-37.

Jenkins H, Holman T, Lyon C, Lane B, Stick R, Hutchison C. (1993) Nuclei that lack a lamina accumulate karyophilic proteins and assemble a nuclear matrix. J Cell Sci. 106:275-85.

Lebel S, Lampron C, Royal A, Raymond Y. (1987) Lamins A and C appear during retinoic acid-induced differentiation of mouse embryonal carcinoma cells. J Cell Biol. 105:1099-104.

Lenz-Bohme B, Wismar J, Fuchs S, Reifegerste R, Buchner E, Betz H, Schmitt B. (1997) Insertional mutation of the Drosophila nuclear lamin Dm0 gene results in defective nuclear envelopes, clustering of nuclear pore complexes, and accumulation of annulate lamellae.J Cell Biol. 137:1001-16.

Lin F, Worman HJ. (1993) Structural organisation of the human gene encoding nuclear Lamin A and nuclear Lamin C. J Biol Chem 268:16321-16326.

Lourim D, Lin JJ. (1992) Expression of wild-type and nuclear localization-deficient human lamin A in chick myogenic cells. J Cell Sci. 103:863-74.

Machiels BM, Zorenc AHG, Endert JM, Kuijpers HJH, van Eys GJJM, Ramaekers FCS, Broers JLV. (1996) An alternative splicing product of the lamin A/C gene lacks exon 10. J Biol Chem. 271:9249-9253.

Manilal S, Nguyen TM, Sewry CA, Morris GE. (1996) The Emery-Dreifuss muscular dystrophy protein, emerin is a nuclear membrane protein. Hum Mol Genet. 5:801-808.

Manilal S, Sewry CA, Man N, Muntoni F, Morris GE. (1997) Diagnosis of X-linked Emery-Dreifuss muscular dystrophy by protein analysis of leucocytes and skin with monoclonal antibodies. Neuromuscul Disord. 7:63-6.

Manilal S, Recan D, Sewry CA, Hoeltzenbein M, Llense S, Leturcq F, Deburgrave N, et al (1998) Mutations in Emery-Dreifuss muscular dystrophy and their effects onn emerin protein expression. Hum Mol Genet 7:855-864.

Manilal S, Sewry CA, Pereboev A, Nguyen thi Man, Gobbi P, Hawkes S, Love DR, Morris GE. (1999) Distribution of emerin and lamins in the heart and implications for Emery-

Dreifuss muscular dystrophy. Hum Mol Genet 8:353-359.

Maniotis AJ, Chen CS, Ingber DE. (1997) Demonstration of mechanical connections between integrins, cytoskeletal filaments, and nucleoplasm that stabilize nuclear structure. Proc Natl Acad Sci U S A. 94:849-54.

Meier J, Campbell KH, Ford CC, Stick R, Hutchison CJ. (1991) The role of lamin LIII in nuclear assembly and DNA replication, in cell-free extracts of Xenopus eggs. J Cell Sci. 98:271-9.

Moir RD, Montag-Lowy M, Goldman RD. (1994) Dynamic proteins of nuclear lamins: Lamin B is associated with sites of DNA replication. J Cell Biol. 125:1201-1212.

Moir RD, Spann TP, Goldman RD. (1995) The dynamic properties and possible functions of nuclear lamins.Int Rev Cytol. 162B:141-82. Review.

Moir RD, Spann TP, Herrmann H, Goldman RD. (2000) Disruption of nuclear lamin organization blocks the elongation phase of DNA replication.J Cell Biol. 149:1179-92.

Mora M, Cartegni L, Di Blasi C, Barresi R, Bione S, Raffaele di Barletta M, Morandi L, Merlini L, Nigro V, Politano L, Donati MA, Cornelio F, Cobianchi F, Toniolo D. (1997) X-linked Emery-Dreifuss muscular dystrophy can be diagnosed from skin biopsy or blood sample. Ann Neurol. 42:249-53.

Morris GE, Manilal S. (1999) Heart to heart: from nuclear protein to Emery-Dreifuss muscular dystrophy. Hum Mol Genet 8:1847-1851.

Murphy J, Crompton CM, Hainey S, Codd GA, Hutchison CJ. (1995) The role of protein phosphorylation in the assembly of a replication competent nucleus: investigations in Xenopus egg extracts using the cyanobacterial toxin microcystin-LR. J Cell Sci. 108:235-44.

Nagano A, Koga R, Ogawa M, Kurano Y, Kawada J, Okada R, Hayashi YK, Tsukahara T, Arahata K. (1996) Emerin deficiency at the nuclear membrane in patients with Emery-Dreifuss muscular dystrophy. Nat Genet. 12:254-9.

Newport JW, Wilson KL, Dunphy WG. (1990) A lamin-independent pathway for nuclear envelope assembly. J Cell Biol. 111:2247-59.

Nigg EA. (1989) The nuclear envelope. Curr Opin Cell Biol. 1:435-40. Review.

Ostlund C, Ellenberg J, Hallberg E, Lippincott-Schwartz J, Worman HJ. (1999) Intracellular trafficking of emerin, the) Emery-Dreifuss muscular dystrophy protein. J Cell Sci. 92:361-372.

Ostlund C, Bonne G, Schwartz K, Worman HJ. (2001) Properties of lamin A mutants found in Emery-Dreifuss muscular dystrophy, cardiomyopathy and Dunnigan-type partial lipodystrophy. J Cell Sci. 114:4435-45.

Ozaki T, Saijo M, Murakami K, Enomoto H, Taya Y, Sakiyama S. (1994) Complex formation between lamin A and the retinoblastoma gene product: identification of the domain on lamin A required for its interaction. Oncogene. 9:2649-53.

Peter M, Nakagawa J, Doree M, Labbe JC, Nigg EA. (1990) In vitro disassembly of the nuclear lamina and M phase-specific phosphorylation of lamins by cdc2 kinase. Cell. 61:591-602.

Pollard KM, Chan EKL, Grant BJ, Sullivan KF, Tan EM, Glass CA. (1990) In vitro posttranslational modification of lamin B cloned from a human T-cell line. Mol Cell Biol. 10:2164-2175.

Pyrpasopoulou A, Meier J, Maison C, Simos G, Georgatos SD. (1996) The lamin B receptor (LBR) provides essential chromatin docking sites at the nuclear envelope. EMBO J. 15:7108-19.

Quinlan RA, Hutchison CJ, Lane EB. (1995) Intermediate filament proteins. Protein Profiles 2:801-952.

Raharjo WH, Enarson P, Sullivan T, Stewart CL, Burke B. (2001) Nuclear envelope defects associated with LMNA mutations cause dilated cardiomyopathy and Emery-Dreifuss muscular dystrophy. J Cell Sci. 114:4447-57.

Rober RA, Weber K, Osborn M. (1989) Differential timing of nuclear Lamin A/C expression in the various organs of the mouse embryo and the young animal: a developmental study. Development 105:365-378.

Rober RA, Sauter H, Weber K, Osborn M. (1990) Cells of the cellular immune and hemopoietic system of the mouse lack lamins A/C: distinction versus other somatic cells. J Cell Sci. 95:587-598.

Sasseville AM, Raymond Y. (1995) Lamin A precursor is localized to intranuclear foci.J Cell Sci. 108:273-85.

Spann TP, Moir RD, Goldman AE, Stick R, Goldman RD. (1997) Disruption of nuclear lamin organization alters the distribution of replication factors and inhibits DNA synthesis. J Cell Biol. 1997 136:1201-12.

Squarzoni S, Sabatelli P, Ognibene A, Toniolo D, Cartegni L, Cobianchi F, Petrini S, Merlini L, Maraldi NM. (1998) Immunocytochemical detection of emerin within the nuclear matrix. Neuromuscul Disord. 8:338-44.

Stuurman N, Heins S, Aebi U. (1998) Nuclear lamins: their structure, assembly, and interactions. J Struct Biol. 122:42-66. Review.

Sullivan T, Escalante-Alcalde D, Bhatt H, Anver M, Bhat N, Nagashima K, Stewart CL, Burke B. (1999) Loss of A-type lamin expression compromises nuclear envelope integrity leading to muscular dystrophy.J Cell Biol. 147:913-20.

Thompson LJ, Bollen M, Fields AP. (1997) Identification of protein phosphatase 1 as a mitotic lamin phosphatase. J Biol Chem. 272:29693-7.

Toniolo D, Bione S, Arahata K. (1998) Emery-Dreifuss muscular dystrophy. In: Emery AEH (ed) Neuromuscular disorders: clinical and molecular genetics. Willey, London, pp87-103.

Toniolo D, Minetti C. (1999) Muscular dystrophies: Alterations in a limited number of cellular pathways? Curr Opin Genet Dev. 9:275-282.

Tsuchiya Y, Arahata K. (1997) Emery-Dreifuss syndrome. Curr Opin Neurol. 10:421-5. Review.

Tsuchiya Y, Haes A, Ogawa M, Yorifugi H, Arahata K .(1999) Distinct regions specify the nuclear membrane targeting of emerin, the responsible protein for Emery-Dreifuss muscular dystrophy. Eur J Biochem 259:859-865.

Ulitzur N, Harel A, Feinstein N, Gruenbaum Y. (1992) Lamin activity is essential for nuclear envelope assembly in a Drosophila embryo cell-free extract. J Cell Biol. 119:17-25.

Ulitzur N, Harel A, Goldberg M, Feinstein N, Gruenbaum Y. (1997) Nuclear membrane vesicle targeting to chromatin in a Drosophila embryo cell-free system. Mol Biol Cell. 8:1439-48.

Van der Kooi AJ, van Meegen M, Ledderhof TM, McNally EM, de Visser M, Bolhuis PA. (1997) Genetic localization of a newly recognized autosomal dominant limb-girdle muscular dystrophy with cardiac involvement (LGMD1B) to chromosome 1q11-21. Am J Hum Genet. 60:891-5.

Vaughan AO, Whitfield WGF, Hutchison CJ. (2000b) Functions of the nuclear lamins. Protoplasma 211:1-7.

Vigouroux C, Auclair M, Dubosclard E, Pouchelet M, Capeau J, Courvalin JC, Buendia B. (2001) Nuclear envelope disorganization in fibroblasts from lipodystrophic patients with heterozygous R482Q/W mutations in the lamin A/C gene. J Cell Sci. 114:4459-68.

Vorburger K, Kitten GT, Nigg EA. (1989) Modification of nuclear lamin proteins by a mevalonic acid derivative occurs in reticulocyte lysates and requires the cysteine residue of the C-terminal CXXM motif. EMBO J. 8:4007-13.

Wallace P, Signer E, Paton IR, Burt D, Quinlan R. (1998) The chicken CP49 gene contains an extra exon compared to the human CP49 gene which identifies an important step in the evolution of the eye lens intermediate filament proteins. Gene. 211:19-27.

Walter J, Sun L, Newport J. (1998) Regulated chromosomal DNA replication in the absence of a nucleus. Mol Cell. 1:519-29.

Way J, Hellmich MR, Jaffe H, Szaro B, Pant HC, Gainer H, Battey J. (1992) A high-molecular-weight squid neurofilament protein contains a lamin-like rod domain and a tail domain with Lys-Ser-Pro repeats.Proc Natl Acad Sci U S A. 89:6963-7.

Weber K, Plessmann U, Ulrich W. (1989) Cytoplasmic intermediate filament proteins of invertebrates are closer to nuclear lamins than are vertebrate intermediate filament proteins; sequence characterization of two muscle proteins of a nematode. EMBO J. 8:3221-7.

Wilson KL. (2000) The nuclear envelope, muscular dystrophy and gene expression. Trends Cell Biol. 10:125-9. Review.

Worman HJ, Feng L, Mamiya N. (1998) Molecular biology and the diagnosis and treatment of liver diseases. World J Gastroenterol. 4:185-191.

Worman HJ, Yuan J, Blobel G, Georgatos SD. (1998) A Lamin B receptor in the nuclear envelope. Proc Natl Acad Sci USA 85:8531-8534.

Yang L, Guan T, Gerace L. (1997a) Integral membrane proteins of the nuclear membrane envelope are dispersed throughout the ER during mitosis. J Cell Biol 137:1199-1210.

Yang L, Guan T, Gerace L. (1997b) Lamin-binding fragment of LAP2 inhibits increase in nuclear volume during the cell cycle and progression into S-phase. J Cell Biol 139:1077-1087.

Yates JR, Warner JP, Smith JA, Deymeer F, Azulay JP, Hausmanowa-Petrusewicz I, Zaremba J, Borkowska J, Affara NA, Ferguson-Smith MA. (1993) Emery-Dreifuss muscular dystrophy: linkage to markers in distal Xq28. J Med Genet.30:108-111.

Yates JR, Bagshaw J, Aksmanovic VM, Coomber E, McMahon R, Whittaker JL, Morrison PJ, Kendrick-Jones J, Ellis JA. (1999) Genotype-phenotype analysis in X-linked Emery-Dreifuss muscular dystrophy and identification of a missense mutation associated with a milder phenotype. Neuromuscul Disord. 9:159-165.

Ye Q, Worman HJ. (1994) Primary structure analysis and lamin B and DNA binding of human LBR, an integral protein of the nuclear envelope inner membrane .J Biol Chem. 269:11306-11311.

Ye Q, Callebaut I, Pezhman A, Courvalin JC, Worman HJ (1997) Domain-specific interactions of human HP1-type chromodomain proteins and the inner nuclear membrane protein LBR. J Biol Chem 272:14983-14989.

Zhang C, Jenkins H, Goldberg MW, Allen TD, Hutchison CJ. (1996) Nuclear lamina and nuclear matrix organization in sperm pronuclei assembled in Xenopus egg extract. J Cell Sci. 109:2275-86.

Zhao K, Harel A, Stuurman N, Guedalia D, Gruenbaum Y. (1996) Binding of matrix attachment regions to nuclear lamin is mediated by the rod domain and depends on the lamin polymerization state. FEBS Lett. 380:161-4.